# Revista Română de Inginerie Civilă

**Indexată în bazele de date internationale (BDI)**

**ProQuest, INSPEC, EBSCO**

**INDEX COPERNICUS, ULRICH'S şi JOURNALSEEK**

**Volumul 8 (2017), Numărul 4**

**MATRIX ROM**
**OP CHIAJNA CP 2**
**077040 – ILFOV**
**Tel. 021 4113617 Fax. 021 4114280**
**e-mail: office@matrixrom.ro**
**www.matrixrom.ro**

## COLEGIUL EDITORIAL



**Revista Română de Inginerie Civilă este publicată și finanțată de editura**
**MATRIX ROM**
**Director executiv: mat. Iancu ILIE**

Online edition ISSN 2559-7485

Print edition ISSN 2068-3987; ISSN-L 2068-3987

# The Living Envelope of the Buildings, Between Myth and Reality

Ana-Maria Dabija

'Ion Mincu' University of Architecture and Urbanism, 18-20 Academiei Street,
Bucharest 010014, Romania

**Abstract**
In the near past we have been shelled with information about the benefits of green roofs, green walls, living walls. New systems and techniques are developing, aiming to provide different solutions, custom or tailored made, to accommodate all our needs for a better indoor or outdoor air, for a less polluted environment, for contributing to the wellbeing of the urban population.
Furthermore, the living layer – the plant layer – brings new, extra functions to the building envelope: energy saving and, on a smaller scale, food.
As we generally look towards the future, it may, occasionally, be interesting to take a glimpse into the past.
A renown Romanian historian, Nicolae Iorga, said that "He who doesn't know the past can neither understand the present nor see the future". He also said "He who forgets does not deserve".
This paper presents the contemporary living components of the building envelope from a historic point of view.

**Keywords:** buildings, green roofs, green walls, living walls

## 1. Back into the history

### *1.1 Roof top gardens*

According to John Magill [1] we owe the modern green roofs to a German roofer, H. Koch. As at the end of the nineteenth century Germany was experiencing rapid industrialization and, in consequence urbanization. One unfortunate consequence of the massive residential building development was the fire hazard of the inexpensive housing, as tar was used to cover the roofs. Koch's idea was to cover the tar with sand and gravel substrate. Shortly, seed colonization occurred and formed meadows. It seems that fifty of these original roofs can still be seen in Germany.

Rooftop gardens were occasionally built in cities in the thirties. In modern architecture, probably the best known example of a historic rooftop garden may be the Rockefeller Center in New York, designed by Raymond Hood (1930 – 1939).

It is stated that the waterproof membrane is still the original one [2], although the life span of such a building component is supposed to last about 15 years, if well designed (the appropriate structure and material), installed and protected (Fig. 1).

Fig. 1. Rockefeller Center Rooftop Gardens. Rian Castillo

The history of the green roofs is, however, very much older, going back almost 3000 years ago, in the ancient city of Babylon. Everyone has heard about the Seven Wonders of the Ancient World: the Hanging Gardens of Semiramis are one of them. And they are also the oldest relic of green roofs.

It may be worth opening a page on Robert Koldewey (10 September 1855 – 4 February 1925). He was the archaeologist who discovered, in the Marduk Ziguratte and the Gate of Ishtar in Babylon (Fig. 2). He also saw in some ruined arches and a well in the neighborhood that seemed to have had a specific functionality, the remains of the famous Hanging Gardens.


Fig. 2. Ancient Babylon, Library of Congress, Public Domain

Strabo describes the Gardens as follows: “The garden is quadrangular in shape, and each side is four plethra in length. It consists of arched vaults, which are situated, one after another, on checkered, cube-like foundations. The checkered foundations, which are hollowed out, are covered so deep with earth that they admit of the largest of trees, having been constructed of baked brick and asphalt – the foundations themselves and the vaults and the arches. The ascent to the uppermost terrace-roofs is made by a stairway; and alongside these stairs there were screws, through which the

water was continually conducted up into the garden from the Euphrates by those appointed for this purpose, for the river, a stadium in width, flows through the middle of the city; and the garden is on the bank of the river" [3]

The most outstanding description was – in our opinion – made by Diodorus Siculus, in the first century B.C [4]: "The park extended four plethra on each side, and since the approach to the garden sloped like a hillside and the several parts of the structure rose from one another tier on tier, the appearance of the whole resembled that of a theatre. When the ascending terraces had been built, there had been constructed beneath them galleries which carried the entire weight of the planted garden and rose little by little one above the other along the approach; and the uppermost gallery, which was fifty cubits high, bore the highest surface of the park, which was made level with the circuit wall of the battlements of the city. Furthermore, the walls, which had been constructed at great expense, were twenty-two feet thick, while the passageway between each two walls was ten feet wide. The roof above these beams had first a layer of reeds laid in great quantities of bitumen, over this two courses of baked brick bonded by cement, and as a third layer of covering of lead, to the end that the moisture from the soil might not penetrate beneath. On all this again earth had been piled to a depth sufficient for the roots of the largest trees; and the ground, when levelled off, was thickly planted with trees of every kind that, by their great size or other charm, could give pleasure to the beholder. And since the galleries, each projecting beyond another, all received the light, they contained many royal lodgings of every description; and there was one gallery which contained openings leading from the topmost surface and machines for supplying the gardens with water, the machines raising the water in great abundance from the river, although no one outside could see it being done. Now this park, as I have said, was a later construction". Diodorus's description was confirmed by archeology of the early twentieth century.

Permanent sprinkling of The Gardens was provided from the Euphrates by a hydraulic pump that led water to the vegetation. Even today it is not clear how the system works but in the ruins which are believed to be of the gardens, three adjacent wells were found, one central, of square shape and two oval, placed laterally, which remind of a hydraulic machine.

### *1.1.1 When were the Gardens built?*

It is said that queen Amytis the wife of Nebuchadnezzar II of Babylon was longing for her homeland - a territory of the contemporary Iran – that was covered with woods. Seeing her sadness the king ordered the builders to re-create a familiar landscape for her: a terraced construction planted and irrigated artificially rose in the city.

According to another legend, the king offered his wife something he already had: the Gardens were there already, built by the founder of Nineveh and Babylon, king Ninius, for his wife, Semiramis. Nevertheless, the Gardens existed and are probably the first example of green roof / rooftop garden in history [5].

### *1.2 Sloped Green Roofs*

Green roofs have been used in the Northern Europe since the viking period [4]: the vernacular Scandinavian dwelling roofs were protected with sod; the vegetation layer has a double role: to ballast the roof shingles against wind and to provide additional thermal insulation (the sod and vegetation layer providing an important thickness) [6].

From the Vikings the technology was adopted on both shores of the Atlantic, sod roofs being seen in Scandinavia, Scotland and France as well as in Canada and French examples of sod roofs, in Newfoundland and Nova Scotia.

Fig. 3 Goats on a sloped roof, at Al Johnson's Swedish Restaurant, Sister Bay WI: Door County Photo Ky

## 2. Green Roofs Today

A roof represents 6-10% of a buildings' costs. Unfortunately in most cases it cannot be seen from the sidewalk or the surrounding buildings (unless it is surrounded by higher natural or built elements). Therefore many roofs develop… ponds or vegetation which, undersigned on purpose, distro the waterproof system of the roof.

Specific layers are provided, in order to discourage the root penetration into the waterproof membrane. At first made of mortar and metal grid, today contemporary materials 9 including recycled ones) allow for the growth media as well as the roof protection, not only to survive but also to protect and emphasize one another.

Seeds are transported by wind and birds and the plants develop wherever they find cracks, sand, earth (Fig. 4). This was how the green roofs appeared in the 1880s and this is still a means for "greening" the roofs, provided that the waterproof layer(s) is well protected against the roots and the chemical aggression produced by the decayed plants.

Fig. 4. Roofs in Bucharest. Photos Alexandru Stan & Ana-Maria Dabija

In other words, one should not be happy if a tree grows on ones' façade or roof, because the roots in fact destroy the structure of the nonbearing elements of the building, that are in its' neighborhood.

The living "layer" is only one component of the mechanical IR and UV protection of the roofing system.

However, the need to provide the additional layers, the nutrients, the appropriate soil type and thickness for the type of plants that are to be installed on the roof led to the legend that these are fastidious systems. Furthermore, if the buildings are not protected against winds and if the trees are high, they may be overthrown. Therefore the designing of rooftop gardens is a delicate approach, that needs a multidisciplinary team, in which the architect, the botanist, the structure engineer must be included.

### *2.1. Green roof types*

According to the type of plants that form the living component, there are three main types of green roofs: extensive, intensive and semi-intensive. The types of plants are strongly connected to the thickness and characteristics of the substrate (soil).

While the extensive roofs require 4-10cm for sedum (mainly) to grow, intensive roofs – rooftop gardens – need thick layers of earth (40 – 100cm) that accommodate the growth of high trees. They are real gardens (as seen in the case of Rockefeller Center –Fig. 1 - or in the Montparnasse Railway Station in Paris - Fig. 5) with alleys, benches and all the necessary street furniture that is needed or requested in a park.

Furthermore, the designing of such gardens is independently carried out for each season, as different plants reach their aesthetic potential in different seasons. Landscape architects and botanists team in this approach.

Fig. 5. Gare de Montparnasse in Paris. Rooftop garden. Photo Ana-Maria Dabija

Like all living creatures plants need time to grow and mature. Therefore it takes time until a green roof reaches its' beauty. It is the case of most pitched roofs where sod and grasses need to grow stronger. Terraces may accommodate container systems, an "all-in-one" product that comes with all components that are requested over a waterproof membrane. They can be easily manipulated and replaced, if necessary.

### 3. Living facades

The concept is not new either. Many country houses (or old urban houses, with courtyards) have beautiful vine vaults that provide "coolth" in the hot summer days. As their leaves fall in autumn, the sun warms the walls in the wintertime… At least this is the romantic approach.

In reality the ivy and vine that cover facades in the historic cities represents vulnerability for the wall. Their "tentacles" thrust in the substance of the walls and, like in the story of the Sleeping Beauty, take over and overgrow the entire building (Fig. 6).

Fig. 6. Building in the "old" Bucharest. Photo Ana-Maria Dabija

Due to the humidity kept by the plants that lean against the facades, the walls may become damp. In order to prevent the accumulation of humidity in the façade, the contemporary living walls are raised on strayed structures. This way the built facade is naturally ventilated, the humidity is removed and the wall has more chances of staying dry. Using the traditional buildings with the climbing ivy as example, the principle of green façade has been developed.

The living walls derive from the ventilated façade systems: panels on a substructure. Panels may be made of wood (that was the beginning), stone, metal, glass and - why not – panels with a growing media that accommodates some types of plants. The growing substrate is usually of a spongy or fibrous origin, that allows the plants to develop roots. There are systems that provide "pockets" with soil, appropriate for indoor, not high walls, in countries with no seismic hazard.

The "inventor" of the green wall is Stanley Hart White, a landscape architect and a professor at the University of Illinois at Urbana – Champaign. It seems that in 1937 he patented the "Botanical Bricks" and in 1938 the "Vegetation Bearing Architectonic Structure and System". In this last patent he describes a method " for producing an architectonic structure-of any buildable size, shape or height, whose visible or exposed surfaces may present a permanently growing covering of vegetation. Another object is to provide a vegetation-bearing structural unit therefor. A further object is to provide such a unit that maybe irrigable, portable and interchangeable. Another object is to provide such a unit-of sufficient flexibility to enable it to be bent, curved or warped into various shapes. Another object is to provide such a unit that may be permanently plant-bearing and plant-nourishing. A further object is to provide fixed, flexible or portable architectonic compounds of such units. Additional objects will more plainly appear from the detailed specification and drawings presented herewith in exemplification but not in limitation of the present invention […] The underlying principle of the present invention is to provide the architectural profession and related industries with an efficient and inexpensive method and means for utilizing a novel medium for ornamental and useful architectonic construction, in various forms of units and compounds having vegetation-bearing surfaces. For example one purpose of these surfaces may be to build decorative backgrounds or screens for masking eyesores or for concealing people or properties - in such a way as to avoid painted camouflage or the heavy cost of ordinary hedges there in a few days, if permanently constructed" [7]. It seems that Stanley Hart White has seen only a tiny part of the potential of the benefits of the living walls .

There is a connection – like in the case of green roofs – between the type of substrate (growing media) and the type of plants. The mastermind in the case of living walls is the botanist who can make arrangements that lead to colours, textures, images.


Fig. 7 Massive greenwall with a Singapore island map. Photo Jonathan Choe

## 3. Benefits of the living envelope

As mentioned before, the first and most important role of the living roof was to protect the membrane from aggressive agents: fire, oxidation, IR,UV, overheating and later to accomplish a mechanical protection.

However, the overall assembly is proven to fulfill other major tasks for the occupants of the building, for the neighborhood and the city.

At the domestic level , the green roof systems provide more thermal comfort as the thickness of the substrate adds to the overall thermal “blanket” but also, a reduced summer energy consumption (as air conditioning is no longer needed). The acoustic comfort in the spaces beneath the roof increases in the case of green roofs.

The process of evapo-transpiration of the plants humidifies the air, decreasing temperature peaks in the summer and landing the dust.

Plants consume carbon dioxide and eliminate oxigen. Plants absorb electromagnetic radiation [8]. Therefore the use of plants at a large scale – a roof scale – contributes to diminishing the pollution of the cities and diminish the heat island effects.

The return of the plants in the cities is also followed by the restoration and diversification of the ecosystems. Plants contribute to the wellbeing and health of all living creatures.

It is obvious why countries like Germany or Switzerland encourage, through legislation, the development of green roofs. Germany for instance has installed a total of 86.000.000 sqm green roofs (data from 2014) [9].One of the advantages of the living and green walls is that in the summer the vegetation shadows the wall while in winter, as the leaves fall, the sun warms the correspondent part of the facade.

The benefits of the green roofs for the building and the city applies to the vertical component of the living envelope as well (green and living walls). Plants filter the air, therefore living walls help in the process of air recirculation in HVAC systems. Their performance is, however, unquantified.

In some countries the plants that are used for the green roofs are not ornamental but different types of vegetables. The concept of urban farm appeared, adding yet an extra function to the envelope: food provider.

Fig. 8. Rooftop farm, Greenpoint. Photo: Lila Dobbs

## References

[1] Magill, John, A History And Definition Of Green Roof Technology With Recommendations For Future Research, Graduate School Southern Illinois University Carbondale April 2011- http://opensiuc.lib.siu.edu/cgi/viewcontent.cgi?article=1132&context=gs_rp

[2] Wark, C.G. Wark, W.W. Green Roof Specifications and Standards. Establishing an emerging technology The Construction Specifier, August 2003, Vol. 56, No.8, in http://www.fussypainting.com/pdf/GreenRoof.pdf

[3] Strabo, Geography XVI.1.5, translation adapted from HL Jones, Loeb edn(1961), in https://en.wikipedia.org/wiki/Hanging_Gardens_of_Babylon

[4] Diodorus Siculus II.10-1-10 in https://en.wikipedia.org/wiki/Hanging_Gardens_of_Babylon

[5] Dabija, A-M, Greening the Buildings. Improving the Built Environment in Romania, International Conference on Smart and Sustainable Built Environment SASBE Sao Paulo Brasil, June 2012, Proceedings, p.211-216

[6] FLL Guideline for the Planning, Execution and Upkeep of Green-Roof Sites.

[7] Patents Vegetation-bearing architectonic structure and system US 2113523 A, in https://www.google.com/patents/US2113523

[8]Parker, D. Barkaszi, S, May/June 1994, Saving Energy With Reflective Roof Coatings, Home Energy Magazine Online, in www.homeenergy.org/archive/hem.dis.anl.gov/eehem/94/940509.html

[9] EFB_WhitePaper_2015

# On the possibility for sea and ocean waves energy utilization by a turbine with fluctuating blades

Emanuil Agontsev[1], Veselin Varbanov[1], Rositsa Velichkova[1], Venelin Makakov[1], Milka Uzunova[2], Iskra Simova[1], Detelin Markov [1]

[1]Technical University of Sofia
Sofia, 1000, 8 Kl.Ohridski Bld
*eagontesev@tu-sofia.bg, rositsavelichkova@abv.bg, iskrasimova@gmail.com, detmar@tu-sofia.bg*

[2]ECAM-EPMI
Cergy-Pontoise France
*m.uzunova@ecam-epmi.fr*

***Abstract.*** *In the current work the operation principle of a new type of water turbine constructed by the authors is presented. This turbine which may utilize the energy of the sea and ocean waves is with fluctuating blades. The kinematic scheme of the turbine is presented and on its basis the main turbine parameters - revs and linear velocity, are defined. In addition to this a test rig for investigation of the turbine parameters is presented.*
***Key words:*** *turbine, fluctuating blades, energy from sea and ocean waves*

## 1. Introduction

Depletion of reserves of conventional energy sources increased the energy prices, environmental pollution from burning of fossil fuels, global warming and climate changes worldwide. This more and more pressing issue leads to two logical starting points:

- Reduction of fossil fuels as an energy source
- Utilization of energy from local renewable energy sources (RES).

Renewable energy is attractive because it is generated with no or only a little pollutants of the environment, available resources are renewed and, in fact, they will never be exhausted. [6, 7]

Basic renewable energy sources are:

- solar energy;
- tidal energy;
- geothermal energy;
- wind energy;
- energy of sea and ocean waves;
- biomass ;

Covering the energy demand of the humanity, and preserving the ecological balance of the earth, is possible only if the inexhaustible energy of the environment is

used. Current work is dedicated to the utilization of the energy of the sea and ocean waves as a renewable energy source. [1,2,3,4,5]

Devices for converting the wave energy along with changes in the level and slope of the surface wave may utilize the changes of the kinetic and potential energy and pressure in the wave. Devices converting wave energy are diverse consistent with typical values that define their work. Some of the main inventions in this direction are listed below:

- Salter's duck (Fig.1) – This is a wave energy device invented by Stephen Salter at the University of Edinburgh during the oil crisis in the 1970s. The device is also known as nodding duck or Edinburg duck. Its shape provides the most efficient extraction of energy from the waves that enters from the left side on figure 1, and thus causing oscillation. The cylindrical opposite side ensures missing of no right wave fluctuations in duck currently stationed around the axis O. The power is taken away from the axis of the oscillating system under conditions of minimal impact. The reflection and transmission of energy and therefore the device has high efficiency in a wide range of wave frequencies.

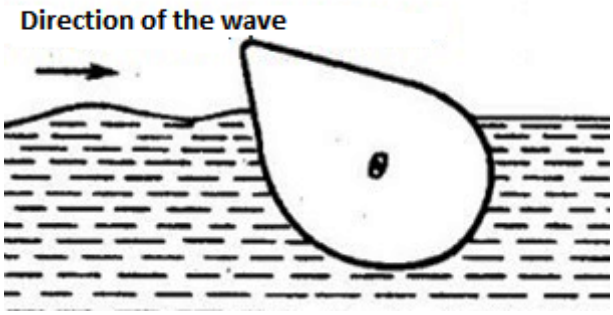


Fig.1 – Stephen Salter's duck (http://greenenergytechnology87.blogspot.bg)

- Oscillating water column (OWC) - When the wave is went on partially submerged hollow tower (Fig. 2), which is open under the wate, the pillar fluid in the hollow is faltered and this exerts pressure of the gas above the liquid. The hollow can be connected with the atmosphere by a turbine. The flow can be adjusted so that it will passes through the turbine in the same direction or to use suitable turbine (eg. Wells turbine).

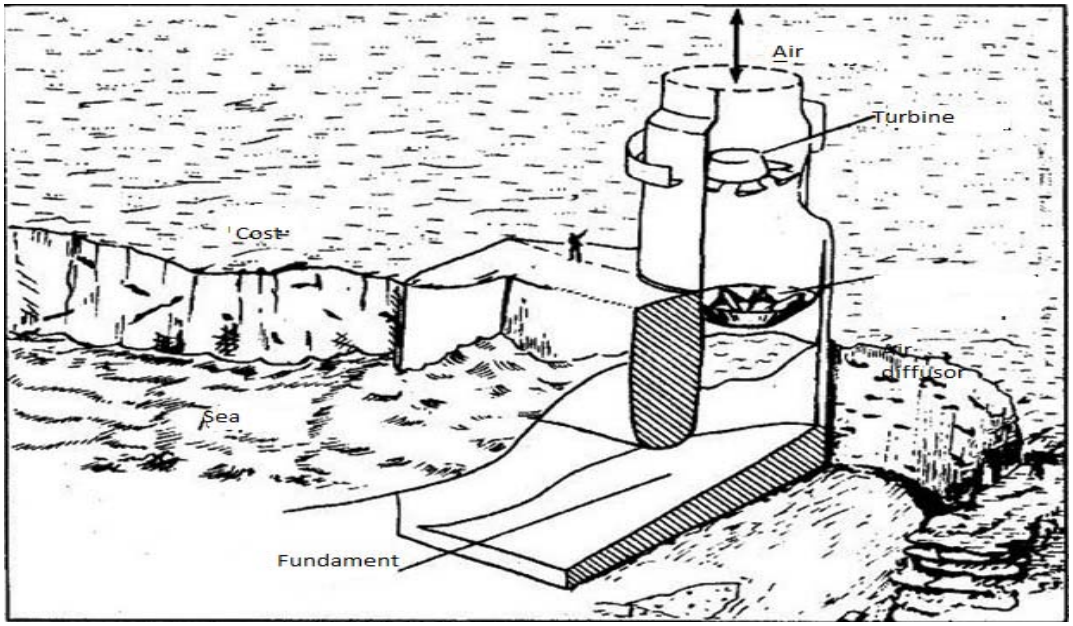


Fig.2 - Oscillating water column (http://greenenergytechnology87.blogspot.bg)

The aim of current paper is to present an idea and model of a test rig for investigation of turbines with oscillating blades that use the energy of the sea and ocean waves. This test rig will be used for experimental study under laboratory conditions.

## 2. Kinematic scheme

The operation principle of the turbine with oscillating blades is the following: the turbine wheel is mounted on a vertical shaft which is connected with a platform located on the free sea surface and moves up and down under the action of the waves. When this movement produces torque relative to the shaft, which is mounted on the wheel, which is transmitted to the platform, the energy (created torque) is utilized. Since the first experiments will be performed under laboratory conditions, it is clearly necessary to adopt the following scheme of movement for obtaining the desired effect: the turbine wheel is immersed in a tank of still water, and the platform to which is attached the shaft carrying the working wheel is forced to perform reciprocating movement up and down thus imitating sea waves.

Such a scheme of movement is achieved through the test rig shown in Figure 3, whose kinematic scheme is shown in Fig. 4. The kinematic scheme enables the necessary kinematic relations to be determined.

Figure 3 shows the construction of the test rig, which consists of the following elements.

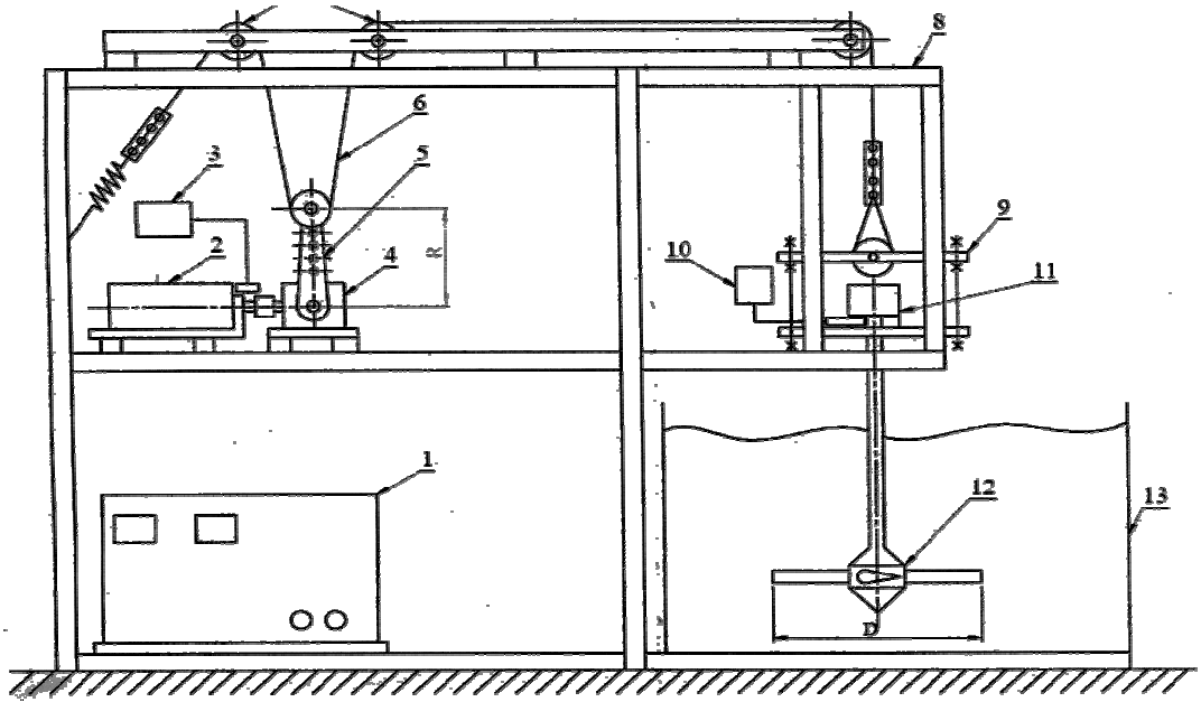


Fig.3 – Construction of the test rig

1 - Rectifier, 2 - DC electric motor, 3 - Tachometer, 4 – Speed Reducer, 5 - Crank, 6 - Lanyard, 7 - Guiding rollers, 8 –Framework, 9 - Mobile platform, 10 - Cyclometer, 11 – Generator, 12 – Impeller, 13 - Water tank

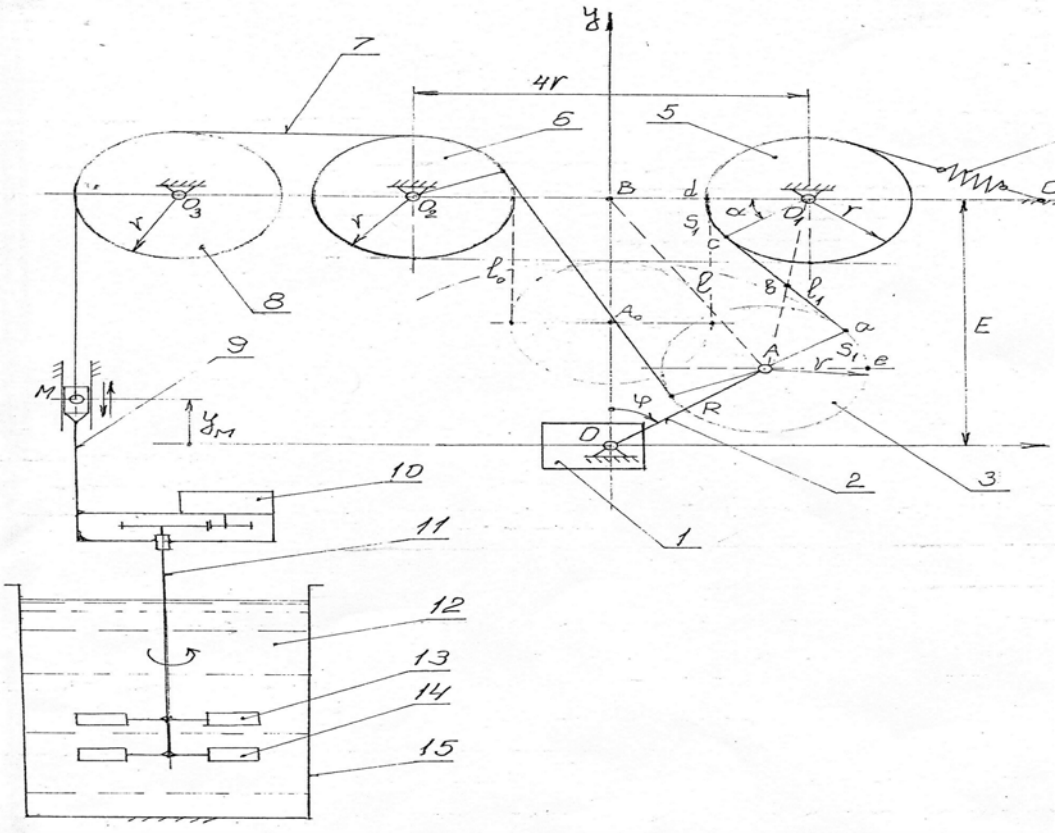


Fig.4 – Kinematic scheme

The operation of the test rig is performed in the following manner: the rectifier 1 supplies the DC motor 2 with electricity and by changing the rotational velocity of the electric motor 2, respectively of the crank 5, which via a system of rollers moves the platform 9 up and down, thereby mimics the behavior of the sea waves. Consequent of the movement of platform 9 the immersed turbine wheel starts to spin, consequently rotating and the shaft on which it is installed. This makes it possible to measure directly the resulting torque and the vertical speed of the impeller (turbine) by the cyclometer 10.

For the proper functioning of the test rig it is necessary to know what is the relationship between the speed of rotation of the crank and the vertical linear speed of the platform.

Referring to the triangle AOB on Fig. 4 formed according to the kinematic scheme, the length $l$ is obtained as a function of the angle $\varphi$

$$l(\varphi) = \frac{R}{\lambda}\sqrt{1+\lambda^2-2\lambda\cos\varphi} \qquad (1)$$

Knowing the kinematic characteristics of the test rig is necessary in order to determine the law of motion of the platform as a function of the speed of the crank. This makes it possible to determine the maximum speed of the crank using these geometric dimensions resulting from the kinematic diagram according to Figure 4. In a consequent analysis and processing it is obtained the law of motion of the platform, expressing the movement of the M point in Fig. 4.

$$y_M(\varphi) = \frac{2R_{kp}}{\lambda}\sqrt{1+\lambda^2-2\lambda\cos\varphi}+\lambda-1 \qquad (2)$$

If the known dependence of drag of streamlined body attached to a freely falling under its own weight wheel and the platform is used, the following relationship can be written:

$$G_{pl} \geq C_x \rho z F_{pl}\frac{v^2}{2} \qquad (3)$$

Once the law of the movement of the platform is known its speed is calculated by:

$$V_M(\varphi) = 2R_{cr}\omega_{cr}\frac{\sin\varphi}{\sqrt{1+\lambda^2-2\lambda\cos\varphi}}, m/s \qquad (4)$$

For the acceleration of the platform is obtained the following:

$$a_M(\varphi) = 2R_{cr}\omega_{cr}^2\frac{\left(1+\lambda^2-\lambda\cos\varphi\right).\cos\varphi-\lambda}{\left(1+\lambda^2-2\cos\varphi\right)^{1,5}}, m/s^2 \qquad (5)$$

Given that the weight of the platform is known along with the speed of movement, the critical speed of the crank, which must not be exceeded, can be determined

$$n_k \leq \frac{15}{\pi R_{kp}}\sqrt{\frac{2G_{pl}}{C_x\rho z F_{pl}}} \qquad (6)$$

Once the main kinematic parameters of the platform motion are known another milestone in the experimental study is to measure the value of the resulting time $M_T$ and the consequent crank revs.

According to Euler the timing $M_T$ is determined by:

$$M_T = \left(P_2 - P_1\right) r_c, N.m \quad (7)$$

## 3. Construction of the test rig

Regardless of the direction of passage of the water through the turbine wheel it is designed so that the direction of rotation of the impeller is not changed. It is known as Wells turbine. These rotors operate continuously under variable speed and pressure of the fluid flow. In order high effectiveness to be achieved, the rotors have to be optimized as the wave energy is not transmitted directly to the turbine wheel. The constructed turbine with fluctuating blades has the advantage that the transmission of the wave power on the turbine wheel is direct, which leads to higher efficiency of the facility. This effect is achieved by constructing the turbine with fluctuating blades as shown in Fig. 5 and 6.

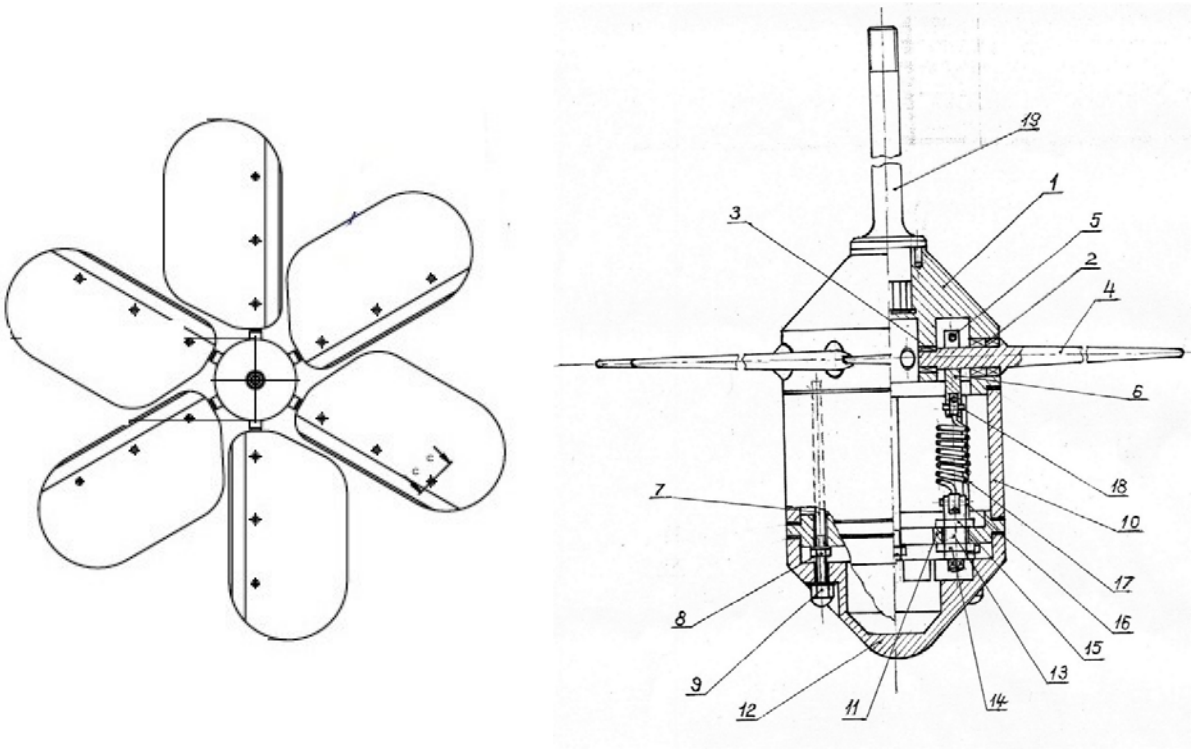


Fig.5 Sketch of the turbine wheel

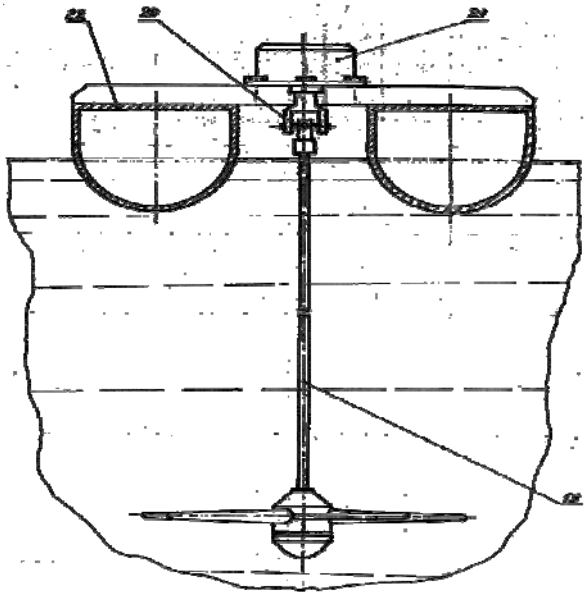

Fig.6 Sketch of the test rig

In the center of the hub of the turbine 1 through a rigid connection is mounted vertical shaft 19 which via a universal connector 20 is connected to an electrical generator 21 mounted on the movable platform 22 situated on the free water surface.

The reciprocation of the turbine wheel takes place in the following way - fig.5. The mobile platform 22 moves up and down with the behavior of a wave, as a result of this movement on the fluctuating blades 4, alternating moments are exerted according to hydraulic axle bearings 2 and 3. These moments are sign varying and are in equilibrium with the spring moments created from the main springs 17. The hydraulic force applied to the static centers of the fluctuating blades 4 have horizontal components which create torque to the vertical shaft in vertical direction.

The moment and the rotation of the hydraulic turbine with fluctuating blades determine the power of the turbine. This power through the vertical shaft 19 and PTO clutch 20 is transmitted to the electric generator 21 located on the platform 22 for utilizing of the received energy.

For a turbine with the following design parameters: $n_{cr} = 60\,\mathrm{min}^{-1}, z = 6,$ $F_1 = 0,026m^2$, $r_w = 0,18m$, $\alpha = 30^0$, $r_d = 0,05m$ experimentally are determined its main parameters, moment, revs and power, by using the equation given above.

$$M_T = 0,494kg.m$$

$$n_T = 18,34\,\mathrm{min}^{-1}$$

$$N_T = M_T.n_T = 0,015kW$$

## Conclusion

The utilization of the renewable energy sources is essential for the growing needs of the modern world. Capturing and converting the energy from sea and ocean waves is just one of the possibilities but with large potential.

The presented hydraulic turbine with fluctuating blades utilizes the kinetic energy of moving water into water courses, either sea or ocean. The movement of large water masses is carried out periodically in the form of tides or lifting and lowering (wave motion of the water), which brings tremendous energy. The hydraulic turbine with fluctuating blades constructed by the authors has the advantage that converts directly the reciprocation of the platform into rotation of the turbine shaft and thus a high efficiency of the hydro-generator would be achieved.

## References

[1] Douglas, C. A., Harrison, G. P., and Chick, J. P. Life cycle assessment of the SeaGen marine current turbine, University of Edinburgh, 2007
[2] French, M.J. On the difficulty of inventing an economical sea wave energy converter: a personal view, University of Lancaster, 2006.
[3] H.YAYuz, A. McCabe, G. Aggidis and M. Widden, Calculation of the performance of resonant wave energy converters in real seas, Proc. IMechE, vol220, Part M pp 117-128, 2006
[4] Rodrigues L., Wave power conversation system for electrical energy production, 2008
[5] S. Walker, R. Howell, Life cycle comparison of a wave and tidal energy device, Proc. IMechW vol. 225 Part M pp 325-337,2011
[6] S. Walker, R. Howell, G. Boyle, Renewable Energy: Power for a sustainable future, Oxford, # edition, 2012
[7] Ts. Petrova, Simulation of the performance of a Stirling engine with kinematic linked piston, Proceeding of Technical university of Sofia, v.63, iss.4,pp.139-147, 2013

# Ship Squat Related Parameters Measurements On Board Training Ship Mircea

Petru Sergiu Șerban[1]

[1]"Mircea cel Bătrân" Naval Academy
Fulgerului 1, 900218 Constanța, Romania
*E-mail: sergiu.serban@anmb.ro*

**Abstract.** *During July – August 2015 sailing ship "Mircea" conducted an international training voyage departing from Constanța, Romania with stopovers in four ports. On this occasion there had been conducted a series of measurements on vessel's draft, water depth below keel and ship's speed when entering and leaving the ports because these areas showed, more or less, the characteristics of restrictive areas that could favor the emergence of squat phenomenon. This paper presents experimental conditions, equipments and methods used on board to determine parameters needed in ship squat calculations. After results interpretation there were identified several conclusions regarding the measurement methods used.*

**Key words:** ship squat, sailing ship, draft, camcorder, depth under keel.

## 1. Introduction

In the last decade it was observed a continuous increase of the main dimensions of certain ships, especially for container carriers, RO-RO vessels and LNG carriers. In opposition, the dimensions of access channels, rivers, canals and harbors where these vessels operate do not increase at the same rate [1].

Therefore, restricted waters impose significant effects on ship navigation. In these situations the ship has to navigate close to the shore and other manmade structures because of limited navigable width. The shallow water and proximity of the sides of the channel affect the ship navigating through the restricted waters. With the presence of a side bank in the vicinity of the hull, the flow is greatly complicated. Additional hydrodynamic forces and moments act on the hull, thus changing the ship's maneuverability. These effects cause errors in maneuvering which can lead to grounding or collision [2].

A phenomenon that occurs on vessels in these areas is ship squat, which may be defined as the sinkage and/or trimming of the ship due to pressure changes along the ship length in shallow waters. Ship to ship interaction or ship to shore is also related to this phenomenon. The trim change can be explained by hydrodynamic interactions between the ship and the bottom due to speed and pressure distribution change. Large and fuller ships such as tankers and bulk carriers should pay extra attention when navigating in restricted waters. The squat effect is directly related to ship dimensions, its speed and water depth [3].

Ship squat phenomenon has been the subject of studies in many ways for a long time. In general, most researches rely on empirical formulas, experimental tools or numerical (Computational Fluid Dynamics) techniques, among which the first two types are more widely used [4].

Scientific research on ship squat was started by *Constantine* (1960), which studied the phenomenon for subcritical, critical and supercritical speeds. In subcritical domain, *Tuck* (1966) demonstrated that in open water conditions of constant depth, the sinkage and trimming of the vessel varies linearly with depth Froude number. This theory was developed by others, such as *Beck* (1975) for dredged channels, *Naghdi* and *Rubin* (1984), *Cong* and *Hsiung* (1991), *Jiang* and *Henn* (2003) or *Gourlay* (2008) [5].

Current researches on this phenomenon are limited to experiments on scale models for an accurate mathematical expression of ship squat. The literature presents various formulas of ship squat, the most commonly used being those of *Barrass* (2004), *Millward* (1992), *Norrbin* (1986), *Hooft* (1974) and *Romisch* (1989) [6].

The aim of the paper is to present experimental conditions, equipments and methods used on board NS "Mircea" to determine parameters needed in ship squat calculations. In summer of 2015 Romanian Naval Academy sailing ship "Mircea" conducted an international training voyage with four ports of call. On this occasion there had been conducted a series of measurements on vessel's draft, water depth below keel and ship's speed when entering and leaving the ports because these areas showed, more or less, the characteristics of restrictive areas that could favor the emergence of squat phenomenon.

| **Nomenclature** | |
|---|---|
| $h$ [m] | water depth |
| $T$ [m] | ship draft |
| $Fr_h$ [dimensionless] | Froude number (water depth dependant) |
| $C_B$ [dimensionless] | block coefficient |
| $A_C$ [m$^2$] | canal cross section area |
| $A_M$ [m$^2$] | area of midship section |
| $S$ [dimensionless] | blockage factor ($A_M/A_C$) |
| $V_K$ [knots] | forward speed of the vessel |
| $S_{max}$ [m] | maximum ship squat |
| $h_{uk}$ [m] | water depth under keel |
| $t$ [s] | moment of time |
| | |
| *Subscripts* | |
| b | bow |
| s | stern |

## 2. Ship squat

The shallow water effect manifests itself typically in the increasing of inertia and damping hydrodynamic forces of the hull, changes in the propeller and rudder operation parameters and their interaction with the vessel's hull. Besides, propulsion in shallow water gives rise to forces acting in a vertical plane and bringing about considerable changes in the vessel's stability and trim. Shallow water also causes significant changes in the vessel's roll/pitch parameters [7].

Squat is the decrease of under keel clearance caused by the movement of the submerged ship's body through water. Compared with the static position, the hull goes deeper into the water and trims for a few degrees.

A moving vessel pushes the water in front of her bow, which must flow back under and at the sides of the ship to replace the volume of water displaced by the ship's hull. In shallow and/or narrow waters the water particles' velocity of flow increases (Fig. 1) which results in a pressure drop, according to Bernoulli's Law. The pressure drop under the ship causes a vertical sinking of the ship's hull and depending on the vessel's block coefficient it will trim forward, aft or will sink deeper on even keel. The amount of all vertical sinking and trim is called ship squat [8].

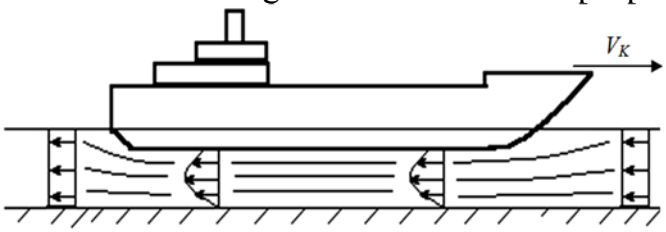


Fig. 1. Distribution of speeds between ship bottom and seabed where $V_K$ is ship speed in knots.

The effect of reduced underwater clearance manifests itself most noticeably by the ratio of water depth $h$ to vessel's draft $T$, $h/T$ is less than 2. The degree of the shallow water effect depends on the vessel's relative speed through the depth Froude number. For Froude number, $Fr_h$, of more than 0.3, the effect of the hydrodynamic forces and squat is significant. The shallow water effect, change of trim and stability and other related phenomena increase dramatically after Froude number $Fr_h$ of 0.8 and reach the maximum at Froude number around 1.0 which corresponds to the "critical" speed [9].

Squat formulas have been developed for estimating maximum ship squat for vessels operating in restricted and open water conditions with satisfactory results. Some have been measured on ships and some on ship models. *Barrass*'s formula [3] is among the most simple and easy to use for all channel configurations. Based upon his research from 1979, 1981 and 2004, the maximum squat formula (Eq. 1) is empirical and it is determined by the block coefficient $C_B$, blockage factor $S$, defined as the ration between mid-ship cross-section area ($A_M$) and canal's cross section area ($A_C$), and ship speed in knots $V_K$:

$$S_{\max} = \frac{C_B \cdot S^{0.81} \cdot V_K^{2.08}}{20}. \quad (1)$$

The main factor is ship speed $V_K$. In this context, $V_K$ is the ship's speed relative to water; therefore, the effect of current/tide must be taken into account.

The value of the block coefficient $C_B$ determines if the maximum squat occurs at bow or stern. Full-form ships produce squat at bow if $C_B$ is greater than 0.7. Fine-form ships with $C_B$ less than 0.7 produce squat at stern. Ships with $C_B$ near 0.7 produce a mean bodily sinkage equal to maximum squat with no trimming effects [10].

## 3. Training ship "Mircea"

Built between 1938 – 1939 at "Blohm und Wöss" shipyard in Hamburg, Germany, "Mircea" is the fourth ship in a series of five of the same type built at the same site, being sister with "Eagle" – USA, "Gorch Foch I" – Germany, "Gorch Foch II" – Germany, "Sagres" – Portugal.

"Mircea" (Fig. 2) is a training class A sailing ship, bark type, having three masts, 44 meters high and 23 sails with a total sail area of 1750 $m^2$. It has the possibility of mechanical propulsion using a controllable pitch propeller driven by the engine. Its sailing vessel body shape is made entirely of metal with massive metal keel. The ship is fitted with solid ballast and the side frames numbering starts from stern to bow with an inter-frame distance of 600 mm for the entire ship's length. The main characteristics are presented in Table 1.

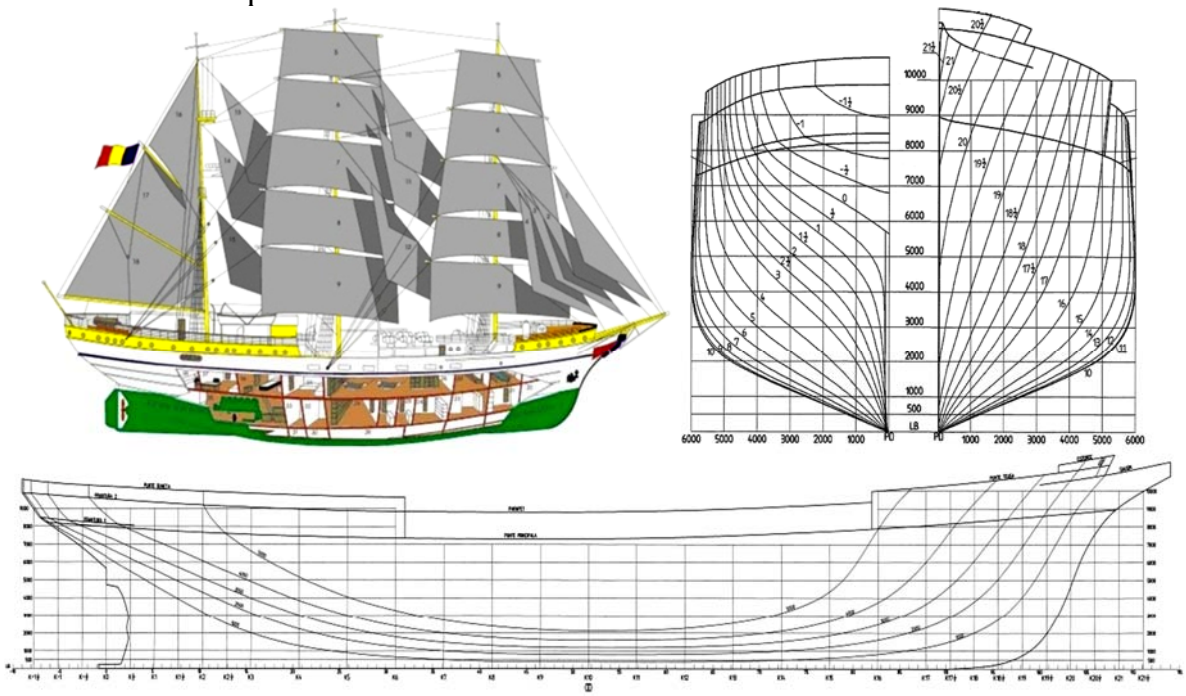

Fig. 2. Sailing ship "Mircea" – body and sheer plans.

Between 1st July and 10th August 2015, Romanian Naval Academy "Mircea cel Bătrân" training ship conducted an international training voyage, departing from port of Constanța, Romania and stopovers in the ports of Civitavecchia (Italy), Barcelona (Spain), Marseille (France) and Bar (Montenegro).

*Table 1*

**Sailing ship "Mircea" characteristics**

| Dimensions | Unit |
|---|---|
| Length over all | 81.6 m |
| Maximum body length | 73.6 m |
| Length between perpendiculars | 62.0 m |
| Beam | 12.0 m |
| Moulded depth | 7.3 m |
| Moulded draft | 5.35 m |
| Block coefficient | 0.486 |
| Gross tonnage | 1312 t |
| Displacement | 1840 dwt |
| Propulsion | 1100 hp MAK diesel engine |
| Speed | 9.5 knots |
| Endurance | 21 days |
| Range | 4000 Nm |

## 4. Measurement methods used

Within port waters, during the entrance maneuver until quay mooring maneuver and during the departure maneuver from harbor, there were performed measurements of closely related parameters to the phenomenon of squat: vessel draft, depth under keel and speed.

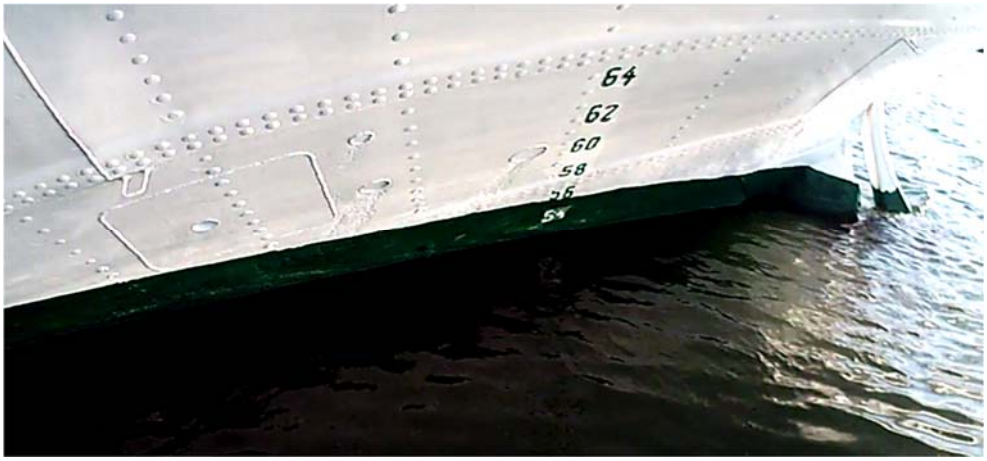


Fig. 3. Stern draft mark on board "Mircea".

On board, the ship's draft is determined by a direct reading of draft marks located at bow and stern on the hull (Fig. 3). Typically, drafts' reading is done before the ship leaves the quayside by direct observation from the shore. When the ship is underway, bow draft is readable on board from forecastle deck, but stern draft cannot be read because the draft scale is not visible from the poop deck. To eliminate this problem and record stern draft variation, the author used a HD Midland XTC 200 720p camcorder mounted on a wooden extending rod, 4 m in length (Fig. 4), fixed to the deck railing.

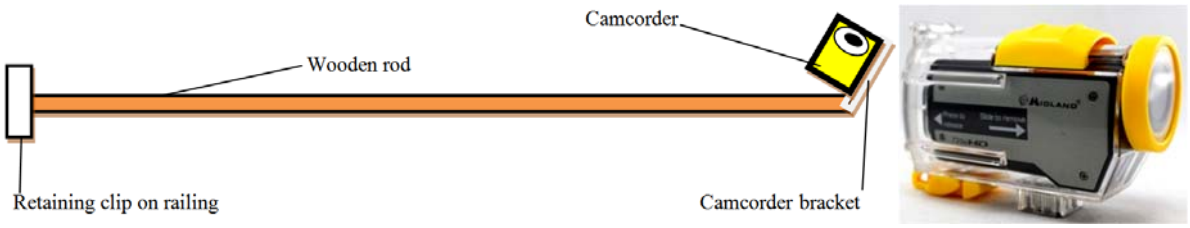


Fig. 4. HD Midland XTC 720p camcorder.

At the same time there were recorded data of depth under keel from Sperry ES 5000 echo sounder fitted on board the ship. It accurately measures depth in shallow or deep waters, having four operating scales ranging from 10 m to 2000 m and displays a seabed depth graph on a LCD display (Fig. 5). For continuous depth recording, the echo sounder enables printing the graph on paper. Thus, the author extracted depth from graphics for different moments in time, which were correlated with the draft recorded on the camcorder.


Fig. 5. Sperry ES 5000 echo sounder.

Vessel's position, course and speed were retrieved electronically from the electronic charts system, which receives this information from GPS.

## 5. Results

For squat, critical speed or depth Froude number calculations, water depth $h$ is necessary and can be obtained by adding the measured under keel depth $h_{uk}$ with average draft $T$. Knowing the bow and stern drafts ($T_b$, $T_s$), the following formula (Eq. 2) was used for water depth:

$$h = h_{uk} + \frac{(T_b + T_s)}{2}. \quad (2)$$

After collecting speed and water depth data from each port and studying draft videos there had been obtained information synchronized in time which are presented in the following figures.

At the entrance, the initial moment $t$ for data gathering was considered, in each case, when the vessel doubled the entry lighthouse of the port and the end of the measurements was considered when the ship speed was 3 knots (1.54 m/s). Reversely, the beginning of measurements was considered when the ship speed exceeded 3 knots and the end when the ship left harbor. Data extraction was done at 30 seconds

intervals. The speed of 3 knots was chosen as the lower limit for readings start/stop because below this speed, the ship moves too slowly and the phenomenon of squat would not occur or would be imperceptible.

### 5.1. Port of Civitavecchia, Italy

In accordance with the ITTC (International Towing Tank Conference) recommendations, a ship is in shallow waters if the ratio between the water depth $h$ and mean draft of the ship $T$ satisfies the condition $1.2 < h/T < 1.5$.

At the entrance to the port of Civitavecchia there were measured depth under keel obtained from the echo sounder, stern draft obtained from video recordings and bow draft from direct observations. Mean draft was calculated with value of 5.35 m, because bow draft was consistently 5.3 m and stern draft varied between 5.35 m and 5.4 m according to analyzed records. Thus, every 30 seconds, there were calculated water depth $h$ (Fig. 6) and the ratio $h/T$. It was noted that this ratio values ranged between 2.68 and 4.27, so it was not within the limits necessary to meet the shallow water condition presented above. The situation was similar at the departure maneuver.

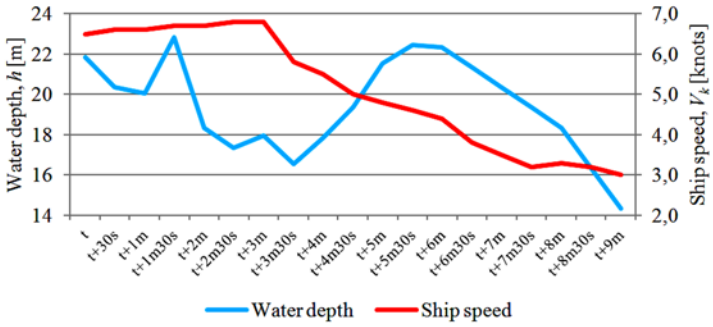


Fig. 6. Civitavecchia - entrance maneuver. Water depth and ship speed.

Total distance traveled when entering port was 1358 m with a maximum speed of 6.8 knots (Fig. 6) and when departing, 1649 m with a maximum speed of 6.9 knots (3.55 m/s).

### 5.2. Port of Barcelona, Spain

When entering Barcelona there were made the same measurements as previous. Mean draft was calculated to 5.325 m as the bow draft was consistently 5.3 m and stern draft varied between 5.3 and 5.35 m. Thus, at each moment of time, there were calculated water depth $h$ (Fig. 7) and the ratio $h/T$ with values ranging between 2.31 and 4.66, which was not within the limits necessary to meet shallow water condition.

If a ship is in open water conditions, there is an artificial boundary port and starboard, parallel to her centreline, beyond which there are no changes in ship speed, ship resistance or in ship squat. This artificial boundary is known as a "width of influence" whose value depends on the type of ship and the block coefficient. Inside

this width of influence when moving ahead, the ship will experience a loss of speed, a decrease in propeller revolutions and also increased squat [3].

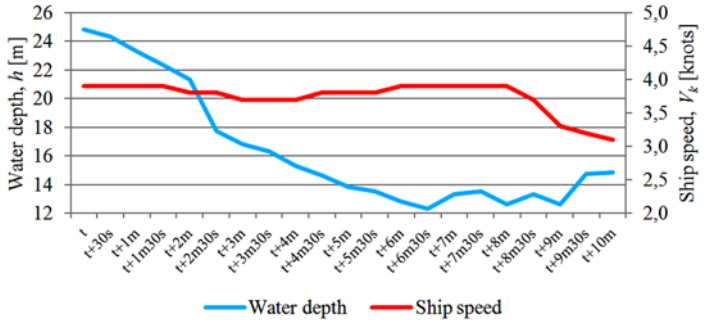


Fig. 7. Barcelona - entrance maneuver. Water depth and ship speed.

For this case, the width of influence was calculated to a value of 216.42 m. Although the vessel moves to the center of the fairway, the width of influence boundaries were violated sometimes by the breakwaters or piers from the harbor, but due to the average low speed of only 3.74 knots, the ship motion was not influenced by the presence of obstacles and squat did not occur. On departure the situation was similar, but *h/T* values ranged between 1.96 and 3.12, but still not sufficient to satisfy shallow water condition.

Total distance traveled when entering port was 1148 m with a maximum speed of 3.9 knots (Fig. 7) and when departing, 1501 m with a maximum speed of 6 knots.

### 5.3. Port of Marseille, France

On entering Marseille there have been made the same measurements as previous. Mean draft was calculated to 5.3 m as the bow and stern draft were consistently 5.3 m. Even so, the ratio *h/T* had values ranging between 2.34 and 2.91 when entering harbor and 2.23 to 4.31 when departing.

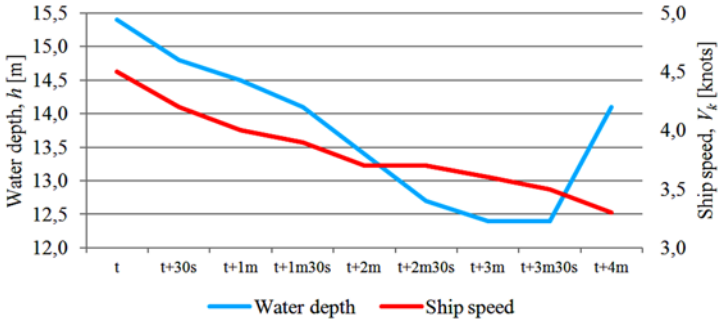


Fig. 8. Marseille - entrance maneuver. Water depth and ship speed.

In this case, the width of influence was 217 m. The width of influence starboard limit was violated on a small portion by the entry dike, but due to average low speed of 3.82 knots the ship motion was not influenced by the presence of obstacles and squat did not occur.

Total distance traveled when entering port was 475 m with a maximum speed of 4.5 knots (Fig. 8) and when departing, 591 m with a maximum speed of 5.9 knots.

### 5.4. Port of Bar, Montenegro

On entering Bar, mean draft was calculated to 5.325 m as the bow draft was consistently 5.3 m and stern draft varied between 5.3 m and 5.35 m. Thus, for every moment of time, there were calculated water depth *h* (Fig. 9) and *h/T* ratio. It was noted that ratio values ranged between 2.99 and 3.62, so it was not within the limits necessary to meet the shallow water condition. On departure, *h/T* values ranged between 2.43 and 3.14.

In this case, the width of influence was 216.41 m. The port artificial boundary of width of influence was violated on a small portion by the entry dike, but due to average low speed of 3.44 knots the ship motion was not influenced by the presence of obstacles.

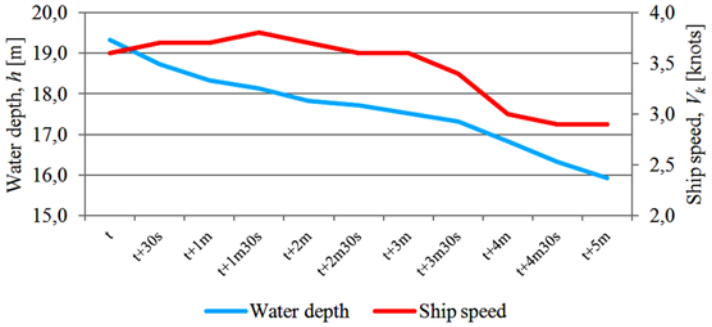


Fig. 9. Bar - entrance maneuver. Water depth and ship speed.

Total distance traveled when entering port was 531 m with a maximum speed of 3.8 knots (Fig. 9) and when departing, 703 m with a maximum speed of 4.3 knots.

## 6. Conclusions

The aim of the paper was to present experimental conditions, equipments and methods used on board NS "Mircea" to determine parameters needed in ship squat calculations. In summer of 2015 Romanian Naval Academy sailing ship "Mircea" conducted an international training voyage with four ports of call. On this occasion there had been conducted a series of measurements on vessel's draft, water depth below keel and ship's speed when entering and leaving the ports because these areas showed, more or less, the characteristics of restrictive areas that could favor the emergence of squat phenomenon.

From the taken measurements and results interpretation there were extracted the following conclusions:

- The only way on board the ship to measure draft is by direct observation of draft marks. Therefore, for the stern draft readings, which are harder to read, it was used a video camera fixed on a wooden extending rod to record draft variation and viewing it afterwards.
- Regarding measuring methods, there have been identified, on board and when compiling data, a difficulty in syncing the draft records with under keel depth graphs from echo sounder and speed obtained from the electronic charts system, because

these information come from different navigation equipments with offset internal clocks.

- Attempts to capture on record a noticeable draft change, which could be attributed to the phenomenon of squat, proved unsuccessful due to unsuitable ship characteristics, slow maneuvering speed and ports not sufficiently restrictive.

Another decisive factor of squat non-occurrence was the variable ship speed on entering and departing maneuvers. In laboratory conditions, experiments on models in towing tanks are made at constant speed over long distances and water depth and canal width are also constant. These conditions favor the squat phenomenon, but in reality full-scale measurements proved to be more difficult to reproduce.

Maximum squat determination for shallow and/or narrow waters remains an important issue for safety of navigation. Masters should know before entering such areas, where and how much the draft will increase to take actions for countering this phenomenon.

## Acknowledgements

The author wishes to express his appreciation to the rector of "Mircea cel Bătrân" Naval Academy, Rear Admiral Professor Engineer, PhD, Vergil Chițac, for the opportunity to participate in this training voyage on board NS "Mircea". Also the author would like to acknowledge the help and support received in this work from commander of NS "Mircea", Capt. (N) Gabriel Moise.

## References

[1] *S. Șerban, C. Katona, V.N. Panaitescu*, Case study of ship to ship interaction using NTPRO 5000 navigational simulator, "Mircea cel Bătrân" Naval Academy Scientific Bulletin, vol. **XVII**, issue 2, 2014, pp. 31-35

[2] *L. Chun-Ki, L. Sam-Goo*, Investigation of ship maneuvering with hydrodynamic effects between ship and bank, Journal of Mechanical Science and Technology, vol. **22**, 2008, pp. 1230-1236

[3] *C.B. Barrass, D.R. Derrett*, Ship Stability for Masters and Mates, 7th ed., Elsevier, Oxford, 2012

[4] *L. Zou, L. Larsson*, Numerical predictions of ship-to-ship interaction in shallow water, Ocean Engineering, vol. **72**, 2013, pp. 386-402

[5] *G. Delefortrie, M. Vantorre, K. Eloot, J. Verwilligen, E. Lataire*, Squat prediction in muddy navigation areas, Ocean Engineering, vol. **37**, 2010, pp. 1464–1476

[6] *M.J. Briggs*, Ship squat predictions for ship/tow simulator, Coastal and Hydraulics Engineering Technical Note, vol. **72**, 2006

[7] *P.S. Șerban*, Case study of ship squat in Sulina channel using NTPRO 5000 navigational simulator, Applied Mechanics and Materials, vols. **809-810**, 2015, pp. 1193-1198

[8] *P.S. Șerban, C. Katona, V.N. Panaitescu*, Ship squat for a theoretical hull model in trapezoidal variable cross-section canal, Conferința tehnico-științifică internațională "Probleme actuale ale urbanismului și amenajării teritoriului" – culegere de articole, vol. **II**, 2014, pp. 201-207

[9] *** Description of Transas mathematical model, 2nd ed., Transas Ltd., Saint-Petersburg, 2011

[10] *P.S. Șerban, C. Katona, V.N. Panaitescu*, The analysis of squat and under keel clearance for different ship types in a trapezoidal cross-section channel, Universitatea Politehnică București Scientific Bulletin, Series D, vol. **77**, issue 3, 2015, pp. 205-212

# Energy efficiency increasing through space management. Case study in an office building

Ioana Udrea[1], Tudor Trita[2], Romeo Traian Popa[3]

[1]ASC-Romania
9 Stefan Marinescu Street, District 6, 060121, Bucharest, Romania
*E-mail: ioana.udrea@asc-ro.com*

[2]ROFMA
47-53 Lascar Catargiu Blvd., District 1,010665, Bucharest
*E-mail: tudor.trita@rofma.ro*

[3]Technical University of Civil Engineering in Bucharest
Polytechnic University of Bucharest, Faculty of Mechanical Engineering and Mechatronics, Thermodynamics Department
313 Spl. Independentei 313, District 6, 060042, Bucharest, Romania
*E-mail: poparomeo@gmail.com*

**Abstract.** *European Directives which establish energy targets for 2020 and 2030 are the main legislation when it comes to reducing the energy consumption of buildings. Energy efficiency is a large field of study, it doesn't mean only energy consumption minimization by improving measures applied to building envelope and its systems. An efficient use of energy and spaces is very important too. Facility Management (FM) is a field of study that considers all the aspects of a building in this regard. Main pieces of software in the field were reviewed in order to find the better software to use for space management analysis. A well known software - ARCHIBUS, that can integrate Building Information Models (BIMs) was chosen. BIMs are files containing physical and functional characteristics of the building and linked data, which can be exchanged or networked to support decision-making. Using a Romanian office building and its digital plans, a BIM has been done. For this BIM, a space allocation in agreement with organizational company structure, with functional company structure and with a Romanian standard, SR 1907-2, relate to design indoor temperature, was done in ARCHIBUS software. From all space classifications the methods of energy improvement are discussed.*

***Key words:*** *energy efficiency, facility management, space structure, ARCHIBUS*

## 1. 1. Introduction

A continued reduction of energy consumption in buildings is required by European Directives, 2010 Energy Performance of Buildings Directive [1] and 2012 Energy Efficiency Directive [2]. The building sector is the main user of energy, with a percent of 40% from Union's final energy consumption. The building energy evaluation is usually made for some design temperatures and by reporting total energy consumption to useful floor area of the building. This approach is very correct and allowed a consensus of all buildings. But the real use of energy and space in building and the people behavior inside it are at least as important as classic building energy assessment. In this regard, Facility Management (FM) is a field of study that considers all the aspects of a building.

According to International Facility Management Association (IFMA) definition, FM is a profession that encompasses multiple disciplines to ensure functionality of the built environment by integrating people, place, process and technology [3]. From the definition given by EN 15221-1 [4], it can be found that FM represents "integration of processes within an organization to maintain and develop the agreed services which support and improve the effectiveness of its primary activities." A good presentation of FM field, its history and a synthesis of new relevant FM papers can be found on European Facility Management Network (EuroFM) [5]. EU FM Coalition [6] is a European organization that emphasizes the importance of energy efficiency in FM in the context of European Directives targets. Romanian Facility Management Association (ROFMA) is an important promoter of Facility Management in our country [7].

In order to realize a building and its space analysis from FM approach the main software in the field were reviewed. FM software helps the facility managers to conduct and optimize their activities. According to an important reviews portal [8], Buildium is a finest choice of property management software, especially for residential properties and associations. It stands out for its clean and easy to navigate interface. Other recommendation is Total Management, a good commercial property management software. One of the best features is the highly customizable dashboard and its optimal multitasking capabilities. From another source of FM software classification [9], it is found DirectLine, a Web-based service that provides solutions management maintenance and inventory cost and that has 25 years of successful implementations. CAFM Explorer software is a product for organizations looking to better utilize space, improve service levels, and tighten cost control. From [9] also, ARCHIBUS software is found, it is presented as a global provider of software and services for real estate, facility, and infrastructure management. In [10] the authors realized a presentation of FM software field and it results that ARCHIBUS is one of the industry's leading software packages. The author mentions also a commercial maintenance management system, IBM - Maximo Asset Management. In [11] the authors present ARCHIBUS as a brand of internationally renowned property management software. ARCHIBUS comprises a space management tool that integrates location tracking and space management capabilities with facilities management

systems or software [12] and it allows users to link design elements, such as furniture, equipment, located in a database with CAD plans of the building [13].

Some of the facility management software, including ARCHIBUS, can integrate Building Information Models (BIMs). Building information modeling is a process involving the generation and management of digital representations of physical and functional characteristics of places. BIM helps us understand the way buildings look, the way they function, and the ways in which they are designed and built. This is a worldwide trend at the moment. BuildingSMART alliance [14] is a North American organization and a council of the National Institute of Building Science that coordinates the creation of tools and standards that allow projects to be built electronically before they are built physically using Building Information Modeling. This organization develops comprehensive norms related to BIM development as United States National CAD Standard [15] and United States National BIM Standard [16]. The FM software that use BIMs implement an IWMS (Integrated Workplace Management System) that get a single, integrated real estate-focused solution that addresses all business domains. The five core functional areas are Space Management, Operations and Maintenance, Real Estate Management, Capital Project Management, Sustainability and Energy Management. Space Management module has features that permits CAD/BIM integration. An IWMS solution is based on a single platform and database repository [17]. Other Facilities Management software use CAFM system that is defined as a combination of Computer-Aided Design (CAD) and/or relational database software with specific abilities for FM [18].

In [19] the relation between BIM and FM software is discussed. Several innovative techniques were used to input the information directly in the BIM model. For this study two FM software were used, ARCHIBUS and FacilityMAX. From [20] it can be found that ARCHIBUS Space Management is the effective way of managing space and to minimize cost wastage and optimize space usage. The optimization of space management contributes to efficiency and success to most organizations. The authors analyze space management, particularly in a Malaysian University. The importance of space management within the meaning and understanding of Facilities Management is highlighted by the authors in [21]. They recommend the best methods for space management to the higher education institutions.

From its good space analysis method and its integration capabilities ARCHIBUS software was chosen for present study.

The aim of this paper is to present a real case of interdisciplinary use of the same BIM. That means a time economy and a systematization of the data and efficient space utilization can be made. More than this, in this study, it is for the first time when a new space classification is realized in ARCHIBUS in order to allocate the design temperatures to the rooms.

## 2. Method

### 2.1. Studied building description

The building chosen for this research is named MultiGalaxy and it is rented by OMV Petrom Global Solutions SRL. The height regime of the building is 3S + P + 9E, its gross area is over 15.000 sqm and the construction year is 2008. MultiGalaxy is an A class office building, according to BOMA [22] and has a very good add on factor 3.7% (difference between the usable area and the rentable area of an office building expressed as a factor of the rentable area). The building has two generators of 700 kW power and last generation security and protection systems. It is provided with curtain walls composed of glass type Guardian and Schuco structure. The HVAC system is realized by a three pipes heating/cooling plant type Sanyo with VRF (Variable Refrigerant Flow) with ecological Freon agent. This kind of system, with three pipes presents the advantage that they can operate simultaneously in heating or cooling regime. The ability to simultaneously heat certain zones while cooling others is realized by a heat recovery system has. The input power of the system is achieved by acting the heating pumps compressors using a thermal engine with gas fuel. This kind of system can be used at nominal capacity for outdoor temperatures up to -21 degree.

Fig. 1. The studied building, MultiGalaxy, rented by OMV Petrom Global Solutions SRL

### 2. 2. ARCHIBUS software description

ARCHIBUS is produced by ARCHIBUS, Inc. of Boston, Mass. ARCHIBUS is a Real Estate and Facilities Management software that offers a variety of platform options to accommodate the organization's needs - from single users within a department to worldwide access via the Internet for every industry. The need to extract, duplicate, or e-mail data and files is eliminated by the new Run Anywhere architecture [23]. ARCHIBUS software is an IWMS platform that permits a workspace customization and a continuous development of the software. As any IWMS, ARCHIBUS integrates

main business domains, but in this research, Space Planning&Management domain presents interest. ARCHIBUS can operate with digital building plans and links them to its database. Thus, a lot of information and classifications related to CAD plans can be made. Any further modifications of the plans will lead to automate database modification. These kinds of space management allow a good and accurate room inventory, employee assignment to organizational space allocation, internally bill departments for their space usage and other benefits.

## 2.3. Spaces assignment

From the definitions related to BIM, in this paper its main definition is considered, "a model that contains characteristics of the building and linked data which can be exchanged". Thus, although, generally BIM refers to 3D models, in this paper, respecting its basic definition, a BIM is used.

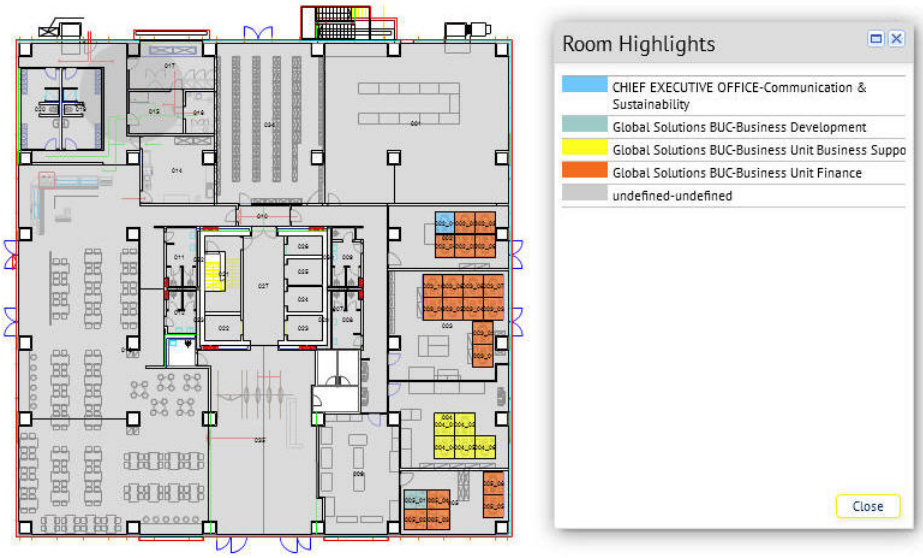


Fig. 2. MultiGalaxy building, groound floor, organizational space structure by divisions

Using ARCHIBUS Smart Client DWG Editor and the MultiGalaxy building floor plans, the rooms surfaces were linked to ARCHIBUS database. Thus, to allocate the building room's spaces to different spaces category was possible. The organizational company structure has a hierarchical model, composed of business units, divisions, departments, offices, and sub-offices. An organizational space structure by divisions can be seen in figure 2. In figure 3, functional structure of spaces according to EN 15221-6 [24] is realized. We need to mention the main international standards used in FM for area and space measurement, BOMA [22] and EN 15221-6. ARCHIBUS software is design to classify the space according to BOMA norm. But in the project where MultiGalaxy building is included, space classification is done using European norm by software customization. According to EN 15221-6 standard the room's areas are classified in primary area, circulation area, technical area, and amenity area (toilets, showers, changing rooms).

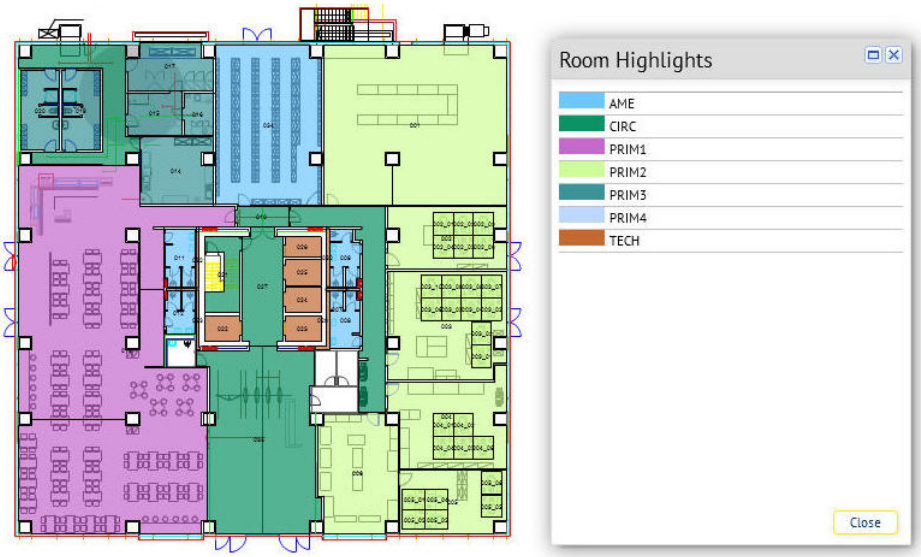


Fig. 3. MultiGalaxy building, groound floor, functional structure of spaces according to EN 15221-6

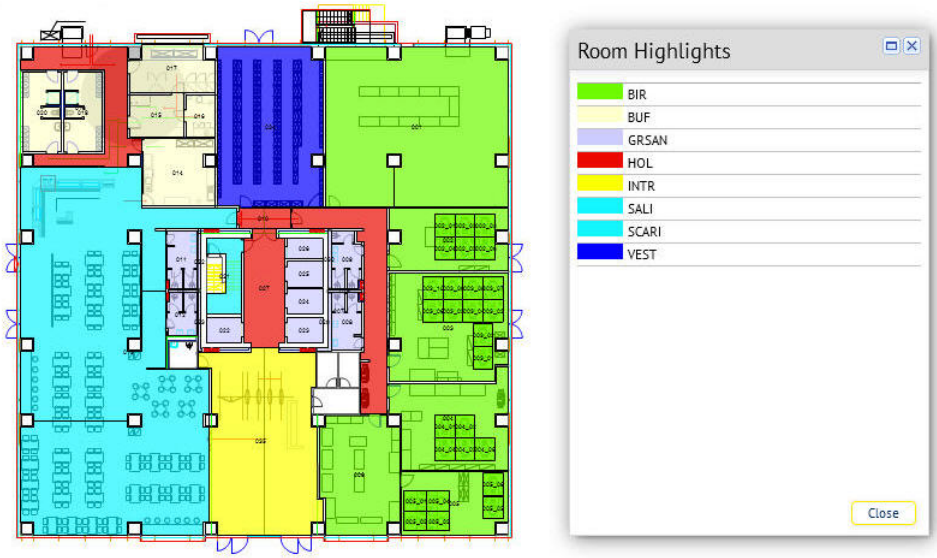


Fig. 4. MultiGalaxy building, groound floor, space structure according to SR 1907-2

In figure 4, a new space classification, according to Romanian norm SR 1907-2 [25] is made. This standard associates a conventional (design) indoor air temperature for each room's type, in residential and nonresidential buildings.

## 3. 3. Results and discussions

The energy consumption in buildings can be reduced by classical method that means modernization solutions of the building and its systems or by rational use of energy and spaces. By rational use of energy it is understood the compliance with comfort temperature requirements, compliance with intermittent heating or cooling program. Where possible, the change of classical comfort temperatures with adaptive comfort temperatures [26] represents a decreasing of energy consumption. And it is not least important the rational use of space that means the reduction of the space allocated to a person. Based on industry studies, many organizations, both public and private sector alike, have been found to underuse office space. And more than this, efficient and effective space usage will be controlled at an expenditure cost and level of productivity [20].

The organizational space structure by divisions can be seen in figure 2. An efficient usage of the spaces is accomplished by employee assignment to the organizational structure of the building. Thus, the energy consumption can be reported to the employee instead of sqm, and it is significantly reduced. In figure 3 a functional classification of the spaces is presented. The space use is carefully watched and the common area, for example, can be reduced and thus, the energy used, reported to sqm of rented area, can decrease.

In figure 4 a space classification according to SR 1907-2 is made; the rooms are grouped according to indoor conventional air temperatures. The room's areas corresponding to different temperatures were exported from ARCHIBUS to EXCEL as xls file. In table 1 the data is systemized and the indoor reduced temperature is computed. This temperature can be used further in energy evaluation programs in order to find energy use for the studied building. Those indoor conventional air temperatures must be the set point temperatures for the HVAC system sensors.

At the end of this paper a comparison between indoor conventional air temperatures proposed by SR 1907-2 indoor comfort temperature recommended by European standard EN 15251 [27] is made. In European standard the temperatures are classified according to comfort category (A, B and C). In EN 15251 the temperatures are structured according to type of building/space and they are not at the same detail level as is SR 1907-2. As can be noticed in Table 1 the mean comfort temperature (for category B) is of 20 ºC in EN 15252 case and the mean reduced (design) temperature is of 18.4 ºC in the case of SR 1907-2.

*Table 1*

**Indoor reduced temperature computation for MultiGalaxy building, ground floor**

| | BIR | HOL | GRSAN | BUF | INTR | SALI | SCARI | VEST | | |
|---|---|---|---|---|---|---|---|---|---|---|
| Supr [$m^2$] | 519.1 | 54.4 | 84.3 | 115.6 | 123.5 | 376.0 | 12.2 | 105.8 | 1390.9 | TOTAL |
| T_i (SR 1907-2)[ºC] | 20 | 15 | 15 | 20 | 12 | 18 | 15 | 22 | 18.4 | T_i_red |
| T_i (EN 15251)[ºC] | 20 | 20 | 20 | 20 | 20 | 20 | 20 | 20 | 20.0 | T_i_comf |

## 5. Conclusions

In conclusion, space management is one of the essential components in FM and in building energy efficiency.
In this paper it is for the first time when, in ARCHIBUS software, such an interdisciplinary space classification is made, all of these classifications are related to energy efficiency in the building. In the project that includes MultyGalaxy building, the possibility of space classification according to European norm EN 15221-6 was made by software customization. A new space classification, accordingly to SR 1907-2 is realized. It can be used in further computations for building energy assessment and for the centralization of room's set point temperatures used by the HVAC system.
For the studied building, a comparison between the indoor conventional air temperatures recommended by Romanian norm and indoor comfort temperatures proposed by European standard was made. A significant difference, of 1.6 ºC can be noticed. Although the EN 15251comfort temperatures are partially transposed in Romanian norm I5 [28] we recommend to update indoor conventional air temperatures proposed by Romanian norm SR 1907 according to our day room types. The indoor air temperature is different from comfort operative temperature and also it is important in design and HVAC set point.

## Acknowledgements

The authors thank to Mr. Dipl. Eng. Mircea Dobre, Department Manager - Facility Services, OMV Petrom Global Solutions SRL for useful information about MultiGalaxy building.

## References

[1] DIRECTIVE 2010/31/EU OF THE EUROPEAN PARLIAMENT AND OF THE COUNCIL of 19 May 2010 on the energy performance of buildings, URL: http://eur-lex.europa.eu/legal-content/EN/ALL/;ELX_SESSIONID=FZMjThLLzfxmmMCQGp2Y1s2d3TjwtD8QS3pqdkhXZbwqGwlgY9KN!2064651424?uri=CELEX:32010L0031, [accessed: March 2015];
[2] DIRECTIVE 2012/27/EU OF THE EUROPEAN PARLIAMENT AND OF THE COUNCIL of 25 October 2012on energy efficiency, URL: http://eur-lex.europa.eu/legal-content/EN/TXT/?qid=1399375464230&uri=CELEX:32012L0027, [accessed: March 2015];
[3] IFMATM, International Facility Management Association, URL: https://www.ifma.org/about/what-is-facility-management, [accessed: March 2016];
[4] EN 15221-1:2006, Part 1: Facility management. Terms and definitions
[5] EuroFM, European Facility Management Network, URL: http://www.eurofm.org/index.php/what-is-fm, [accessed: March 2016];
[6] EU FM Coalition, European Facility Management Coalition, URL: http://www.eufm.org/, [accessed: May 2016];
[7] ROFMA, Asociatia Romana de Facility Management, URL: http://www.rofma.ro/, [accessed: April 2016];
[8] Property Management Software Reviews, URL: http://www.reviews.com/property-management-software/, [accessed: March 2016];

[9] Capterra, Top Facility Management Software Products, URL: http://www.capterra.com/facility-management-software/, [accessed: March 2016];
[10] Lee S., Akin O., Augmented reality-based computational fieldwork support for equipment operations
and maintenance, Automation in Construction 20 (2011) 338–352;
[11] Chang C. Y., Tsai M. D., Augmented reality-based computational fieldwork support for equipment operations and maintenance Knowledge-based navigation system for building health diagnosis, Advanced Engineering Informatics, Volume 27, Issue 2, April 2013, Pages 246–260
[12] Floris, D.B. and Puybaraud, M.C., Space management system and method, US Patent App. 12/397,143, Google Patents, 2009, https://www.google.com/patents/US20090300174
[13] Hart, M.A., Office management solution, US Patent App. 12/009,327, Google Patents, 2008, https://www.google.com/patents/US20080183483;
[14] Building SMART alliance – a council of the National Institute of Building Sciences, URL, http://www.nibs.org/?page=bsa, [accessed: March 2016];
[15] United States National CAD Standard – V6, a product of National Institute of Building Sciences buildingSMART alliance;
[16] National BIM Standard – United States, an initiative of the National Institute of Building Sciences buildingSMART alliance;
[17] Planon – Aim for the Optimum, URL: http://planonsoftware.com/uk/glossary/cafm/, [accessed: March 2016];
[18] WBDG – Whole Building Design Guide, a program of the U. S. National Institute of Building Sciences, URL: https://www.wbdg.org/om/cafm.php, [accessed: March 2016];
[19] Sattenini A., Azhar S., Thuston J., Preparing a Building Information Model for Facility Maintenance and Management, Proceedings of the 28th ISARC, Seoul, Korea, p. 150-155
[20] Ibrahim I., Yusoff W. Z., Sidi N. S. S., Space Charging Model: Cost analysis on classrooms in higher education institutions, Procedia - Social and Behavioral Sciences 28 (2011) 246 – 252
[21] Ibrahim I., Yusoff W. Z., Sidi N. S. S., A Comparative Study on Elements of Space Management in Facilities Management at Higher Education Institutions, 2011 International Conference on Sociality and Economics Development IPEDR vol.10 (2011)
[22] Office Buildings: Standard Methods of Measurement - English Version (ANSI/BOMA Z65.1—2010)
[23] Zawadski C., 2010, Latest Version of ARCHIBUS Software Helps Reduce Carbon Footprint and Lower Real Estate, Infrastructure, and Facilities Management Costs, URL: http://archibus.com/press-release/1114/, [accessed: March 2016];
[24] EN 15221-1:2006, Part 1: Facility management. Area and Space Measurement in Facility Management
[25] SR 1907-2/1997 – Romanian Norm, Heating systems. Conventional calculation indoor temperatures;
[26] de Dear, R. J., Brager, G. S., and Cooper, D., Ashrae rp-884; Developing and adaptive model of thermal comfort and preference. Technical report, The American Society of Heating, Refrigeration and Air-Conditioning Engineers, Inc., and Environmental Analytics, editor. Atlanta, 1997
[27] EN 15251:2007, Indoor environmental input parameters for design and assessment of energy performance of buildings addressing indoor air quality, thermal environment, lighting and acoustics. Brussels: CEN (European Committee for Standardization);
[28] I5:2010 - Standard for the design, execution and operation of ventilation and air conditioning systems, approved by Order of the Minister of Regional Development and Tourism no. 1659 of 22 June 2011, published in the Official Gazette of Romania, Part I, no. 504 bis of July 15, 2011

# Restoring the coil pipe thermal insulation layer from the defective fuel system locator. Technological conditions

Bogdan Corbescu[1], Dumitru Puiu[1], Tiberiu Gyongyosi[1], Valeriu Nicolae Panaitescu[2]

[1] Institute for Nuclear Research
Pitesti, Romania
*E-mail: bogdan.corbescu@nuclear.ro*

[2] Politehnica University, Bucharest,Romania
Bucharest, Romania
*E-mail: valeriu.panaitescu@yahoo.com*

**Abstract.** *A technology for restoring the coil pipe thermal insulation layer from the defective fuel system locator that reduces heat loss inside the moderator tank involves pneumatically transferring the thermal insulation powder inside the confined space between the coil pipe and the inner/outer walls of the equipment. Applying this technology aims to shorten the intervention, and more importantly, without replacing the equipment by cutting and restoring the connection pipes. The article briefly describes the problem generated by thermal insulation aging and establishes the technological conditions for its restauration, followed by a description of the device. It later establishes an operating pressure and presents a solution for the injector design followed by result analysis and conclusions.*

**Key words:** coil pipe, thermal insulation, aging, grain, pneumatic transfer

## 1. Introduction

The Defective Fuel System Locator at the CANDU reactor other than supervising the fresh nuclear fuel reload, identifies the primary heat transfer circuit cooling loop into which the case and fuel bundle defect occurred.

The Defective Fuel System Locator sequentially monitors primary cooling agent samples from each reactor fuel channel assembly in order to detect the flow of thermal neutrons. For each of the fuel channels, a sampling route made out of pulse pipe starts from the feeder's exit toward a serpentine pipe (which is a component of an assembly) that is mounted in moderator tank. The coil pipe enter-exit assembly is achieved by applying an approved welding process.

Into each tank filled with cooling water moderator there is a number of flooded coil assemblies mounted vertically in a stable and known geometric configuration, up to the mounting plate. They are fastened with screws to the cover of the tank.

Each coil assembly is composed of an upper and a lower coil, tightly encapsulated between an inner and an outer tube and insulated with mineral powder

compacted by a mechanical vibration process. Inside the inner tube a hollow central tube is welded coaxially on a mounting plate to probe using the flow detector. Between the central and the annular ring there is an annular volume of cooling water, demineralized water from the moderator tank.

At the top of each moderator tank, over the sampling routes, a trolley moves carrying the probing mechanism which is equipped with flow detectors. The Defective Fuel System Locator functions (including probing mechanism) are controlled by a process computer.

The process of localizing defective fuel is extremely complex and highly depends on the reactor operating conditions (power, number of circulation pumps in operation, specific flow distribution on each of the channels ...).

Repairing a coil pipe assembly which is mounted inside the moderator tank requires interrupting the heat transport water flow through the sampling pipes that connect two fuel channel assemblies and coil pipes but also the return line connecting the coils to the exit feeders (near an output collector). Applying this technology is difficult considering that besides the problem of obtaining the necessary approvals, it also requires a period of time in order to prepare and make the intervention which must be established after conducting a simulation for the entire operation on a scale model and also a radiation exposure dose received by the working personnel. On the other hand, this intervention would require repairing the damaged thermal insulation and reintegrating the coil pipe assembly to the circuit thus aiming to reduce the environmental impact, activities which extend the planned shutdown time of the plant.

Applying a restoring technology to the thermal insulation directly on the spot shortens the time of the intervention and reduces the dose of radiation exposure for the personnel involved.

The article briefly describes the problem generated by thermal insulation aging and establishes the technological conditions for its restauration, followed by the results and few conclusions.

## 2. Analysis of the problem posed by thermal insulation aging

Inside the moderator tank chamber and the Defective Fuel System Locator mechanisms, excessive humidity during inactivity periods (between scans) can lead to the humidification of the coil pipe assembly thermal insulation. The damage suffered by the ceramic plugs that close the in/out sampling paths inside the coil pipe assembly due to restricted dilatations favor an increase of the thermal insulation powder humidity.

When scanning, thermal insulation temperature exceeds 100˚C, therefore water infiltrated inside the layer is vaporized. Water vapors on their way out of the mounting plate through the protection tubes inevitably carry particles from the thermal insulation, a mineral powder of mostly extremely fine grain (<< 50 μm).

Mass transfer thus triggered inside the coil pipe assembly thermal insulation during scanning is a proper aging mechanism. Because of the scarcity of water absorbed from the ambient, mass transfer damages the insulation by transporting mineral powder particles from outside the equipment.

Accidental water absorption can accelerate the aging process, inevitably leading to the loss of the thermal insulation in the upper coil. Damage to thermal insulation in the upper coil increases water temperature inside the moderator tank.

In such a situation characterized by accelerated aging damage to the coil assembly thermal protection can embitter the scanning conditions due to higher water temperature inside the moderator tank, much above the alarm level. Note that the waiting period between scans can increase such as a process duration restriction may be necessary or even prevent scanning.

For normal operating conditions we calculated the medium heat flows distributed on a coil pipe (in the two moderator tanks TK1 and TK2): QSTK1 and QSTK2. Assuming that losing the thermal insulation only affects the cooling water inside the moderator tank TK1, the difference between the obtained values is ~ 18 w.

This means that during the scans conducted inside the moderator tank TK1 on cooling water we have a permanent water heating source ~ 3 w greater than the one in TK2.

For a normal scan conducted in normal operating conditions during a period of time ($t_s$), the cooling water temperature inside the TK1 moderator tank reaches $T_2$ by applying the formula:

$$T_2 = \frac{P_1 \cdot t_s + m \cdot c \cdot T_1}{m \cdot c} \qquad (1)$$

For the second moderator tank (TK2), in the same conditions we got a temperature $T_2$ ~ 1˚C lower. Apparently, the difference is extremely low but in order for the cooling water in TK1 to reach initial scanning temperature (Ti) it is necessary to remove heat, which requires a 210 minutes (3h and 30 minutes) waiting period.

In case the ventilated air coolant fails, water temperature inside TK1 would increase by ~ 27˚C surpassing the value set for the security of the neutron flow detectors used during scanning. This involves stopping the scanning process after approximately half of the normal scanning process (½ $t_s$).

In order to reduce the cooling water temperature by ~ 20˚C, it would be necessary for the additional cooling system in TK1 to work continuously at least 3 times during normal scanning process.

For such a situation, repairing the damaged thermal insulation for each pipe coil is mandatory. Repairing the thermal insulation for a coil assembly involves reintroducing mineral powder used as a thermal insulator through one of the coil assembly protection tubes and filling up the space used for insulation.

## 3. Technological condition for repairing the thermal insulation

A suitable solution for all geometrical configurations revealed when uncovering the moderator tank requires using a device for injecting mineral powder (used as a thermal insulator) directly through the protection tube. This solution involves transporting mineral powder in a fluidized layer through hot air, which will later be transferred by an injector successively through the protection tubes into the annular space between the coils and the inner walls of the exterior and interior tubes. Access inside the protection tubes would thus be facilitated, and the intervention period would be considerably reduced, [2].

The idea of introducing mineral powder (used as a thermal insulator) through hot air injection is original and suitable for pneumatically transferring powder with a grain size below 50 μm (pneumatic transfer is usually realized for powder with a minimum of 100 μm grain size).

The ceramic powder injector assembly that was initially designed as an experimental model will be comprised of a working chamber that will accommodate a predetermined amount of mineral powder (used as a thermal insulator) and a powder injector. These two basic subassemblies were joined after a number of experiments by a hose used for transporting a mixture of mineral powder and air compatible with the opening between the protection tube and the coil assembly sampling route. In further experiments we attached an electrical heater subassembly mounted directly on the upper enclosure (part of the working chamber) outer wall, and a feeding device provided with a vibrator for discharging the powder mounted on top of the working chamber.

The supply of mineral powder will be achieved in stages when the pneumatically transported volume will not be enough to restore the insulation.

## 4. Enclosure description. Setting the operating pressure

The work chamber is for streamlining the mineral powder. The working chamber is made out of two chambers (upper and lower) and has a porous plate used as a separation plane. The plate is attached at the upper end of the lower chamber from the upper chamber; its mounting element is a control ring and a sealing gasket.

The lower enclosure is also called pressure chamber because, when the porous plate is charged with extremely fine powder, the pressure in the chamber starts to increase until it reaches the maximum value given by the static pressure of instrument air network. Laterally, near the bottom of the lower enclosure is the instrumental air input zone.

The lower chamber's height is $h_1$, [m], its interior diameter: $D_i$, [m] and its pressure chamber volume: $V_{cp}$, [m3].

The upper chamber's height is $h_2$, [m], its interior diameter: $D_{is}$, [m] and its pressure chamber volume: $V_{is}$, [m3].

The enclosure lid represents the parting plane of between the upper chamber and the powder injector, and between the upper chamber and the filter agent supply device.

As a condition of priming the fluidization process, we can use the granular layer porosity: ε and calculate the packing density $\rho_u$ for the fixed layer of powder initially introduced inside the upper chamber working using the formula, [1]:

$$\rho_u = (1-\varepsilon)\cdot\rho \qquad (2)$$

- $\rho$ - mineral powder density

For the upper chamber volume $V_{is}$, for the filling density $\rho_u$, the fixed powder layer volume is reduced to $V_S$, [$dm^3$].

The quantity of the powder inserted at the start of the experiment is calculated, [1]:

$$M_i = \frac{\pi \cdot D_i^2}{4}\cdot h_3 \cdot \rho \qquad (3)$$

- $h_3$ - height of the fixed mineral powder layer which was initially inserted inside the chamber

After inserting the instrumental air and priming the fluidized bed, the amount of powder $M_S$ remaining in the fixed layer from the upper chamber is calculated (for an ε granular porosity), [1].

$$M_S = V_S^{'} \cdot \rho_u \qquad (4)$$

The amount of powder driven by the air flow, $M_a$, [1]:

$$M_a = M_i - M_S \qquad (5)$$

The fixed layer height becomes $h_3$' [dm].

The working pressure of the instrumental air entering inside is established early in the process to value that exceeds the critical pressure, a value that should provide porosity on the fixed layer in order to prime the fluidized bed. From this moment on, it is considered that the instrumental air speed velocity reaches the value required by the upward solid particles movement inside the layer.

The technological fluidization process uses a poly-dispersed system and will face inevitable problems of multiphase fluid dynamics, which include [1]:

- Volume elements' layer movement;
- Energy transfer from the insufflated air towards the solid particles;
- Transfer of impulses between the particles through impact;
- Mass transfer (upward particle transfer inside the layer).

The fluidized bed that we want to obtain is a non-adiabatic heterogeneous system formed by turbulent pulsation blast air through continuous solid particles entrained in a lurching.

One issue would be to find the optimum speed onto which the air flow does not cause granules separation inside the layer according to their weight, but to lead them directly, either individual or in compound on an ascension, so that when discharging the air through the injector and later through the flexible line, the air-solid particles is kept in a continuous column, without solid particles clusters.

## 5. Operating mode elements of calculation

Research regarding the flow of a fluid environment through a fixed granular layer have shown the existence of mixture currents, upward currents intersected by solids particles free falling back inside the layer in freefall, currents of fluid that surround the particles infiltrating their pores. For the calculation, we are assuming that we are only dealing with spherical particles of an average diameter, d [mm]. In this case, the particle volume is V [$mm^3$], and the area surface is A [$mm^2$]. The equivalent diameter of the porous channel, dec:

$$d_{ec} = 4 \cdot \frac{V}{A} \text{ , [mm]} \quad (6)$$

The specific area, $a_0$:

$$a_0 = \frac{A}{V} \text{ , [m}^{-1}\text{]} \quad (7)$$

The working area specific surface:

$$A_{in} = \frac{\pi D_i^2}{4} \text{ , [m2]} \quad (8)$$

For an air flow of $Q_1$, [$m^3/s$], we can calculate the average velocity, $w_1$:

$$w_1 = \frac{Q_1}{A_{in}} \text{ , [m/s]} \quad (9)$$

With these known elements, we can calculate the Reynolds number value:

$$\mathrm{Re}_1 = \frac{w_1 \cdot d}{\nu_{g100}} \quad (10)$$

$\nu_g$ is the kinematic viscosity of the preheated dry air at t = 100˚C, [3]

For $Re_1$<0.1 there is no drive flow of solid particles, so it is not necessary to calculate the slipping velocity inside the layer, wec. For Reynolds numbers lower than 0.1, the flow near the surface of the sphere is different than the symmetrical flow around it [1]. For a $Q_2$ air flow we obtain the medium particle velocity:

$$w_2 = \frac{Q_2}{A_{in}} \text{ , [m/s]} \qquad (11)$$

We continue by calculating $Re_2$. For the average equivalent velocity:

$$w_{ec} = \frac{w}{\varepsilon_{ec}} c \text{ , [m/s]} \quad (12)$$

For $Re=Re_{ec}/2>0.1$, the inertial terms start to deform the flow symmetry through the porous channels and a boundary layer detachment takes place behind the solid particle so that the air flow drives upswing particles. Airflow and particle ascension inside the layer are related to a laminar flow into which particles float, raise and descend inside the layer on short distances.

In the event that we have no airflow, the scope will fall freely in a fluid (air + solids) estate viscous. The criterion of Archimedes (the solid phase) for this situation, is calculated by formula, [1]:

$$Ar_S = \frac{g \cdot d^3}{\nu_{100}^2} \cdot \frac{\rho_S - \rho_{g100}}{\rho_{g100}} \qquad (13)$$

For Re<0.2 there is laminar flow at a drag coefficient Cx = 24 / Re, Archimedes criterion is calculated using the equation:

$$Ar = \frac{3}{4} \cdot \mathrm{Re}^2 \cdot C_x(\mathrm{Re}) \qquad (14)$$

In order for the sphere to float without falling or ascending inside the layer, a turbulent regime is required that is characterized by Re ≥ 20. The minimum critical fluidization speed in the laminar domain (Re <10) is calculated using the equation (M. Leva):

$$w_{cr} = \frac{0{,}005 \cdot d^2 \cdot g\left(\rho_S - \rho_{g100}\right) \cdot \varepsilon_{cr}^2}{\mu_{g100} \varphi^2 \left(1 - \varepsilon_{cr}\right)}, [1]$$

d = $d_{ec}$, for polydisperse systems;

$\varepsilon_{cr}$, macroscopic porosity at the critical expansion of the granular layer;

$\mu_g$, gas dynamic viscosity at 100˚C, Ns / $m^2$, [3];

$\varphi$, solid particle geometrical form factor; $\varphi = \frac{d_{ec}}{d}$ .

The critical Reynolds number is calculated using the critical interpolation formula (15) which applies for both the laminar and the turbulent regimes.

$$\mathrm{Re}_{cr} = \frac{Ar_S}{150\frac{1-\varepsilon_{cr}}{\varepsilon_{cr}^3} + \frac{1{,}75}{\varepsilon_{cr}^3}\cdot Ar_S} \qquad (15)$$

The floating speed is an important gas dynamic characteristic of a mass of solid particle, located in a stream of air:

$$w_{pl} = \sqrt{\frac{4}{3}\frac{g\cdot d_{ec}}{\rho_{g_{100}}\cdot C_f}\left(\rho_S - \rho_{g_{100}}\right)} \qquad (16)$$

$C_f$ - solid particle coefficient of dynamic gas resistance

for $10^{-4} < \mathrm{Re} \le 0.4 \ldots 2$, $C_f = C_x = \frac{24}{\mathrm{Re}}$ , [1].

Reynolds number for flotation:

$$\mathrm{Re}_{pl} = \frac{w_{pl}\cdot d_{ec}}{\nu_{g_{100}}} \qquad (17)$$

From the graph Li = f ($A_rS$) for polydisperse systems whose granules have regular (>1mm) dimensions and high densities (fig.1), we note that the number of Archimedes (for the solid phase) should vary between 17 and $5\cdot10^5$. In conclusion, in our case, for pneumatic transport it is preferable to test the model and to obtain real dynamic gas data for the desired regime using powder with granulation between 0.003 and 0.050 and a reduced density ($\rho_S$, [Kg/$m^3$]) as a thermal insulator.

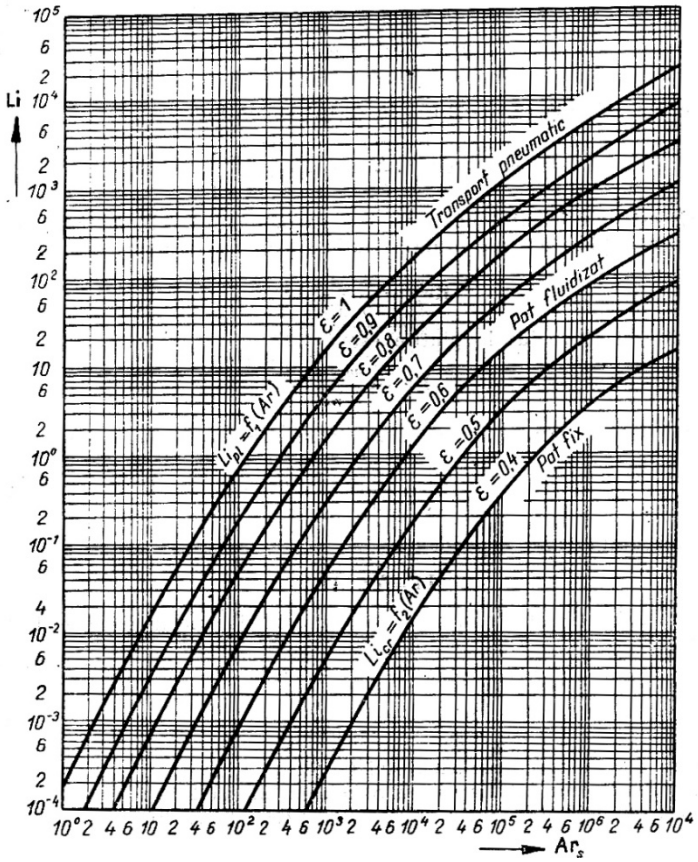


Fig. 1. Li = f (ArS)

## 6. The chosen solution for the design and production of the injector

The injector, an experimental model was designed in a constructive version into which we can change the sequential expansion nozzle geometry and the geometry of the mixing chamber.

For the dimensional computation of the experimental model, we used a simplified calculation model used for wet steam into which we have replaced the sizes characteristic to wet steam with parameters characteristic to the powder - hot air mixture.

The injector, an experimental model was designed and built so as within the test program it would be possible to:
- replace the nozzle;
- modify the nozzle position relative to the mixing chamber entrance;
- modify the mixing chamber length;
- modify the rate of the air flow entering the mixing chamber.

## 7. Results

Excessive humidity inside the moderator tank chamber and the damage that occurs to the ceramic plugs used for closing the input and output of the sampling routes inside the coil assembly, due to the prevented expansions, favors a water absorption increase inside the thermal insulation of the coil (upper and lower).

The temperature inside the coil assembly thermal insulation when scanning the fuel bundles reaches the temperature of the primary heat transport agent that crosses the coil (upper and lower). Water absorbed inside the coil thermal insulation boils instantly and the resulted vapors also inevitably drive extremely fine-grained mineral powder particles (<< 50 μm) spreading them inside the chamber.

Insulation deterioration leads to a water temperature increase inside the moderator tank while scanning fuel channels which finally reaches alarm threshold.

Normally in such a context, between scans, additional water cooling inside the moderator tank would be enough that later during the scanning process, the water temperature should not reach the alarm threshold. In case of ventilated air coolers failure, the situation gets complicated because during scanning, moderator tank water temperature rather quickly exceeds the value set for the security of the neutron flux detectors, thus imposing to stop the scanning process. In order to resume the scanning process, reducing the temperature value for the water temperature inside the moderator tank requires too much time for it to be considered.

In such a case, it is necessary that the coil assembly thermal insulation is rebuilt. Applying this rebuilding technology directly on site (on the moderator tank) would shorten the time of intervention and accordingly, reduce the dose of radiation exposure received by the personnel involved.

We presented the technological restoring condition for the thermal insulation. Such a technique involves using a mineral powder injection device (which will be used as a thermal insulator) directly through the coil assembly protection tube. The idea of injecting mineral powder through hot air is original and suitable for the pneumatic transport of powder with a grain size below 50 μm.

The ceramic powder injector assembly was designed as an experimental model. Its components are a working chamber, an injector and a hose compatible with the space between the sampling route ant the protection tube of the coil assembly.

The working chamber is strictly used for the technological mineral powder fluidization process. It consists of two stacked enclosures (upper and lower) separated by a porous plate. Instrumental air enters the lower chamber (also called pressure chamber) through its side.

The two chambers were sized through calculus so that for a certain instrumental air working pressure, a big part of the powder layer originally introduced inside the upper chamber will be found in the fluidized bed. From there on the air airflow velocity must not cause grain separation inside the layer according to their weight, instead, it must lead them directly, either individual or in compound on an ascension movement towards the injector. It must be a continuous process so that an air discharge through the injector will maintain the air and solid particles mixture in a continuous column without solid particles clusters throughout the entire length of the hose to the inside of the coil assembly. We presented the computing elements of the working regime necessary to ensure the continuity during the experiment.

Priming the fluidized bed and the process continuity was achieved by heating the instrumental air passing through the fixed bed of powder above the porous plate.

The solution for the design and production of the injector was based on the simplified calculations used for wet steam and corresponded to the demands resulted from the experiments.

The experimental ceramic powder injector assembly (fig. 2) was developed and used during few experimental campaigns and was improved accordingly in order to achieve the requirements, [4].

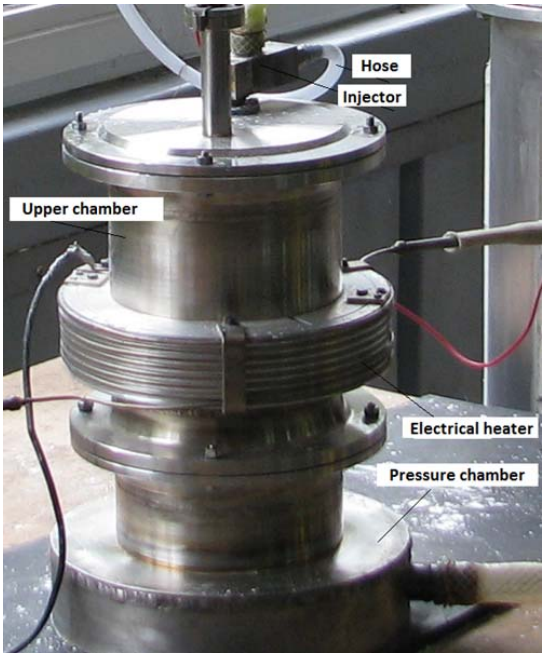


Fig. 2. Experimental ceramic powder injector assembly

## 8. Conclusions

- damage to the coil assembly thermal insulation during the fuel channels scanning process increases the water temperature inside the moderator tank until it nearly reaches alarm threshold;
- in case of accidental damage to the ventilated air coolers, the situation gets complicated because during scanning, moderator tank water temperature would exceed the value set for the security of the neutron flux detectors, thus imposing a stop to the scanning process;
- such a case would require a coil assembly thermal insulation repair;
- applying a technology to restore the damaged insulation for the coil assembly directly on site (on the moderator tank) would shorten the time of intervention thus reducing the radiation exposure dose for the personnel;
- the technological conditions for rebuilding the thermal insulation led to designing and building a ceramic powder injection assembly based on the idea of introducing mineral powder (as a thermal insulator) through hot air injection (given that the powder grain is less than 50 μm);
- priming the fluidized bed and the pneumatic transport continuity was achieved by heating the instrumental air passing through the fixed bed of powder above the porous plate;
- the experimental ceramic powder injector assembly was developed and used during few experimental campaigns and was improved accordingly in order to achieve the requirements

## References

[1] C.Mihaila, Procese termodinamice în sisteme gaz-solid şi aplicaţiile lor în industrie, Editura Tehnica Bucuresti, 1982.
[2] T. Gyongyoşi, S.Valeca, H.Iorga, Dispozitiv de refacere a stratului de izolaţie termică la ansamblul serpentine tanc moderator SLCD, prin injectare de pulberi ceramice. Model experimental, R.I. 7349 / 2005.
[3] M.G. Pop, A.Leca, I. Prisecaru, C. Neaga,..., Îndrumar. Tabele, nomograme şi formule termotehnice, Editura Tehnica Bucuresti, 1987.
[4] T.Gyongyosi, D.Puiu, Gh.Deloreanu, Încercări de formare a jetului de pulbere ceramică utilizând ansamblul injector, model experimental (în prima variantă). Etapa III.R.I. 8547 / 2009.

# Modeling of hazards in room with AB-rechargeable batteries

Rositsa Velichkova[1], Ivan Antonov[1], Milka Uzunova[2], Iskra Simova[1], Kamen Nikolov [1]

[1]Technical University of Sofia
Sofia, 1000, 8 Kl.Ohridski Bld
*rositsavelichkova@abv.bg,mfantonov@abv.bg,iskrasimova@gmail.com, kamen.nikolaev.nikolov@abv.bg*

[2]ECAM-EPMI
Cergy-Pontoise France
*m.uzunova@ecam-epmi.fr*

***Abstract.*** *In current work a numerical modeling of hazards in room with AB-rechargeable batteries is presented. The numerical modeling is done once with the integral method as well as via computer simulation with commercial software package Fluent. A comparison between the obtained numerical results is made and appropriate conclusions for the contaminants in the room are formulated.*
***Key words:*** *numerical simulation, computer simulation, CFD, integral method, pollutants*

## 1. Introduction

Air contaminants indoors can be classified as primary or secondary ones. The main pollutants are substances directly emitted into the atmosphere from the source. The main primary pollutants that are known to cause damage in concentrations that are high enough are as follows:

- Carbon compounds such as CO, $CO_2$, $CH_4$, and Volatile Organic Compounds (VOCs);
- Nitrogenous compounds such as NO, $N_2O$ and $NH_3$;
- Sulphur compounds such as $H_2S$ and $SO_2$;
- Halogen compounds such as chlorides, fluorides and bromides;
- Particulate matter (PM) (PV or "aerosols"), or in solid or liquid form, which usually are classified into these groups based on the aerodynamic particle diameter.

Sulphur compounds are responsible for the traditional winter smog of sulphur. These anthropogenic contaminants sometimes can reach lethal concentrations in the atmosphere, as for example during the infamous case in London in December 1952.

Secondary pollutants are not emitted directly from the source; rather they are formed in the atmosphere from primary pollutants (known as "precursors"). The main secondary pollutants that cause damage in high enough concentrations are as follows:

- $NO_2$ and $HNO_3$ who are formed by NO;

- Ozone ($O_3$), formed by photochemical reactions of nitrogen oxides and VOCs;
- Sulphur acid droplets formed by $SO_2$ and drops of nitric acid formed by $NO_2$;
- Sulphate and nitrate aerosols (e.g., ammonium sulphate and ammonium nitrate) formed from reactions of drops of sulfuric acid and nitric acid respectively with droplets of $NH_3$;
- Organic aerosols formed by VOCs.

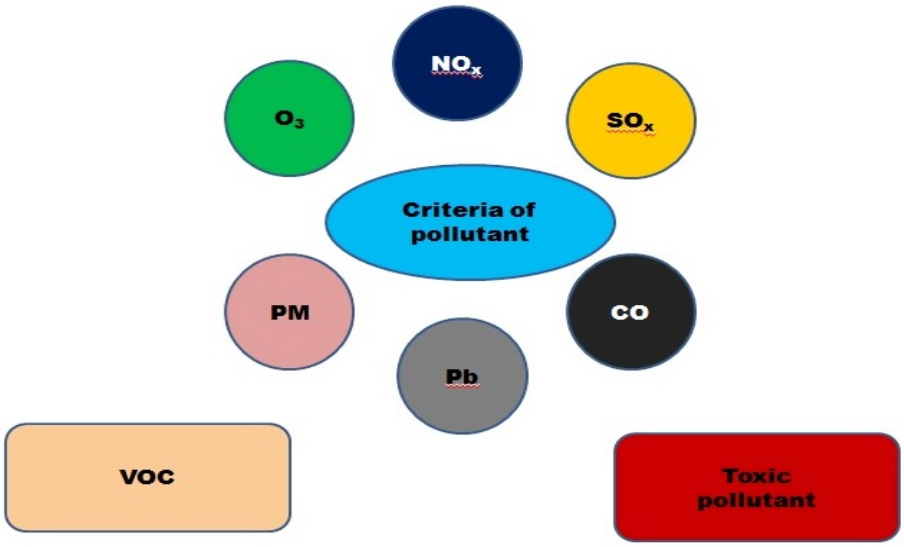


Fig.1 –Pollutants criteria

## 2. Mathematical model of the flow based on Lagrangian method

Discharge of pollutants (dust, liquid "drops", aerosols, etc.) in the working environment can be approximated to a vertical non-isothermal two-phase flow. Due to the temperature difference between the vertical jet and the ambient temperature an Archimedes force will occur. Of course, it is possible the forced vertical flow of contaminants to flow at a temperature close to that of the medium. However, for general solution non-isothermal nature of the flow will be considered.

The non-isothermal nature of vertically transmitted flow requires knowledge of buoyancy (Archimedes) force which is calculated by the expression:

$$dF_A = -\left[\int (\rho - \rho_{ok})\, g df\right] dx \qquad (1)$$

The system of equations of motion of the two phases is as follows:

$$\frac{\partial}{\partial x}\left[y^j U_g \rho_g\right] + \frac{\partial}{\partial y}\left[y^j V_g \rho_g\right] = 0 \qquad (2)$$

$$\frac{\partial}{\partial x}\left[y^j U_p \rho_p\right] + \frac{\partial}{\partial y}\left[y^j V_p \rho_p\right] = 0 \qquad (3)$$

$$\left[y^j U_p\right]\frac{\partial \chi}{\partial x}+\left[y^j V_p\right]\frac{\partial \chi}{\partial y}=-\frac{\partial}{\partial y}\left[y^j \chi V'\right]-\overline{\chi V_p'} \qquad (4)$$

$$\left[y^j \rho_g U_g\right]\frac{\partial U_g}{\partial x}+\left[y^j \rho_g V_g\right]\frac{\partial U_g}{\partial y}=-\frac{\partial}{\partial y}\left[y^j \rho_g \overline{U_g' V_g'}\right]-F_x y^j-\left(\rho_2-\rho_g\right)\pi g y^{2j} \qquad (5)$$

$$\left[y^j \rho_p U_p\right]\frac{\partial U_p}{\partial x}+\left[y^j\left(\rho_p V_p+\overline{\rho_p' V_p'}\right)\right]\frac{\partial U_p}{\partial y}=-\frac{\partial}{\partial y}\left[y^j \rho_p \overline{U_p' V_p'}\right]+F_x y^j \qquad (6)$$

$$\begin{aligned}&\left[y^j \rho_g U_g\right]\frac{\partial h_g}{\partial x}+\left[y^j \rho_g V_g\right]\frac{\partial h_g}{\partial y}=-\frac{\partial}{\partial y}\left[y^j \rho_g \overline{h_g' V_g'}\right]-\\&-\left[y^j \rho_g \overline{h_g' V_g'}\right]\frac{\partial U_g}{\partial y}-Q y^j+F_x y^j\left(U_g-U_p\right)+F_y y^j\left(V_g-V_p\right)-\sum_{i=1}^{3}\overline{F_i' V_{pi}'}\end{aligned} \qquad (7)$$

$$\left[y^j \rho_p U_p\right]\frac{\partial h_p}{\partial x}+\left[y^j\left(\rho_p V_p+\overline{\rho_p' V_p'}\right)\right]\frac{\partial h_p}{\partial y}=-\frac{\partial}{\partial y}\left[y^j \rho_p \overline{h_p V_p'}\right]+Q y^j \qquad (8)$$

$$p=\chi R T_g \qquad (9)$$

In two-phase vertical non-isothermal jets forces of interfacial interactions are decisive in their solution with implementation of the two-fluid circuit - without considering them it is not possible to create mathematical models of two-phase turbulent flow. Determining the impact of the forces of interfacial interaction on the development of the two-phase flow is a necessary element in the creation of numerical models.

The motion of a single particle impurity described by the method of Lagrange leads to an equation of the following type:

$$\sum_{i=1}^{N}\overrightarrow{f_i}=\overrightarrow{f_A}+\overrightarrow{f_S}+\overrightarrow{f_T}+\overrightarrow{f_G}+\overrightarrow{f_{TM}}$$

Then the implemented revisions and laying described in [7] lead to the following equation of the seventh order of the speed of the gas phase:

$$A\overline{U_{gm}^*}^7+B\overline{U_{gm}^*}^6+C\overline{U_{gm}^*}^5+D\overline{U_{gm}^*}^4+E\overline{U_{gm}^*}^3+F\overline{U_{gm}^*}^2+G\overline{U_{gm}^*}+H=0 \qquad (10)$$

The equation is solved by the method of Newton-Rapshan successively and defines the basic parameters of the flow.

$$\overline{U_{pm}}=L_{11}+L_{12}\overline{\rho_{gm}}\,\overline{U_{gm}^*}^2+L_{13}\overline{\rho_{gm}}\,\overline{U_{gm}^*}+L_{14}\overline{\rho_{gm}}+L_{15} \qquad (11)$$

$$\overline{T_{pm}}=e^{\frac{\left(\bar{x}-\bar{x}_0\right)}{L_{106}}}\left(\overline{T_{p01}}+L_{97}\right) \qquad (12)$$

$$\overline{T_{gm}}=L_{94}+L_{95}\overline{T_{pm}} \qquad (13)$$

$$\overline{R_u} = L_4 + L_3 F_x \left( \frac{\overline{U_{pm}} - \overline{U_{gm}}}{\overline{U_{pm}^2}} \right) \quad (14)$$

$$\overline{R_p} = \frac{R_u}{Sc_t} \qquad (15)$$

$$\overline{R_T} = \frac{R_u}{\mathrm{Pr}_t} \qquad (16)$$

In this section is given the mathematical model of the flow and its solution using intregral method.

**3. Numerical analysis of vertical non-isothermal jet flow modeled in a confined space**.

In this section numerical analysis of vertical non-isothermal stream is presented and the modeling phase of the flow in a confined space in particular. Here the initial conditions, the velocity, the temperature and the boundary thicknesses within the boundary layer are listed.

The numerical study is conducted under the following initial conditions: $U_{g0} = U_{p0} = 3m/s$; $T_{g0} = T_{p0} = 303K$; $D_p = 10\mu m$; $y_0 = 0,5m$

On Fig. 2 the distribution of the velocity of the gas phase and the phase of impurities are shown. The graph demonstrates that the velocity along the height of the room almost does not change and the jet reaches the batteries which are situated on the floor as fast as desired.

Fig. 3 shows the temperature distribution of the gas phase and the phase of the impurities along the height of the room. It can be seen that the change in temperature is not significant.

Fig. 4 illustrates the distribution of the three boundary thicknesses of the boundary layer- respectively for impurities Rp, temperature Rt and velocity Ru. The graph concludes that the temperature thickness is greatest, followed by the velocity and impurities' one is the smallest $R_t > R_u > R_p$. Due to $R_t > R_u$ presence of diffusion of heat from the stream to the external environment is observed. Considering that Rp is the smallest value, diffusion of impurities out of the jet is not expected. This is a very significant technology result in the evacuation of impurities from the working environment.

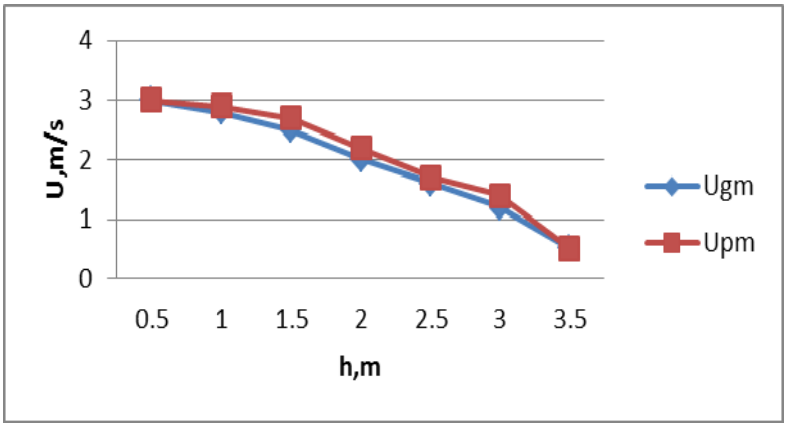


Fig. 2– Distribution of velocity of gas phase and phase of impurity

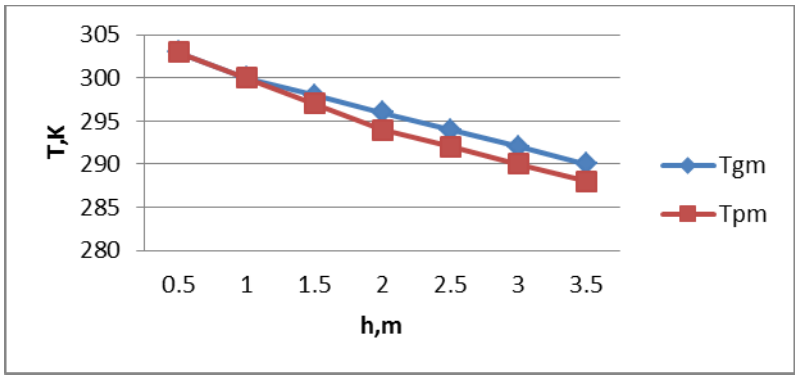


Fig.3– Distribution of temperature for gas phase and phase of impurity

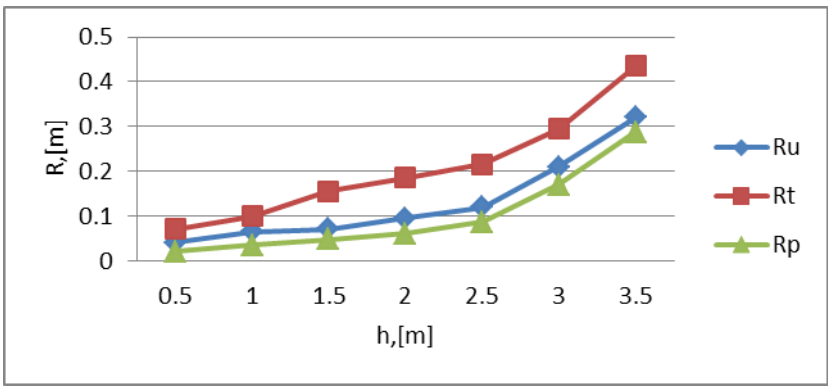


Fig.4. – Distribution of boundary layer thicknesses Ru, Rt and Rp

In section three is given the numerical results for velocity and temperature for both phase. Also is shown the distribution for three boundary layer thicknesses Ru, Rt and Rp.

## 4. Computer simulation of a room with AB- rechargeable batteries

The same scenario of a ventilated room with AB-rechargeable batteries is modeled and simulated by commercial software package Fluent.

The geometry of the room with AB-rechargeable batteries is shown on Fig. 5.

The aim of the computer simulation is to show the distribution of the temperature and velocity field in order to make a comparison between the data obtained by Fluent and results for the velocity and temperature obtained by the Integral method.

For the numerical simulation a relatively simple geometry of the room considered is built, using Fluent's pre-processing panel Gambit. It consists of a rectangular room with AB-rechargeable batteries ordered in rows and situated on the floor. The numerical grid is generated with Gambit's meshing tools and consists of four control volumes. At this stage the boundary conditions are defined as well.

For the 3D computer simulation a pressure based solver is used. The turbulent model chosen for the simulation is based on the Reynolds averaged Navier-Stokes equations. Standard k-ε turbulent model is selected. Appropriate boundary conditions are defined.

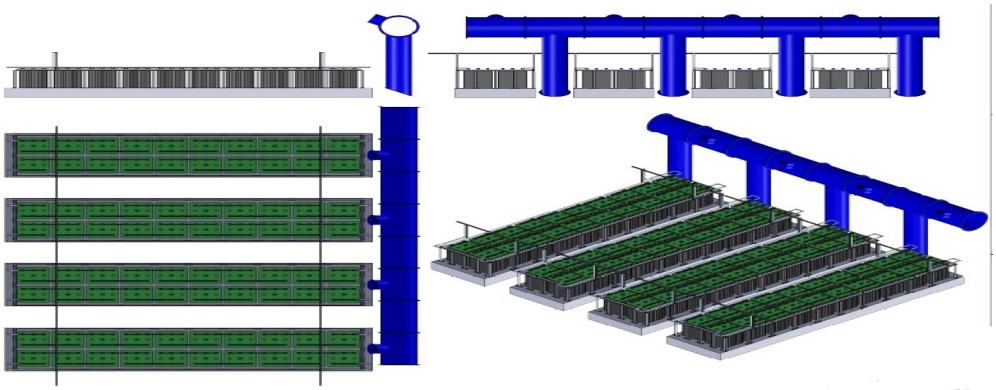

Fig.5 Geometry of the ventilated room with AB-rechargeable batteries

The visualization of the results of the numerical solution is made in the software FLUENT. In it is defined the parameters of the boundary conditions and turbulent models are selected. On the following figures are presented visualizations of the velocity and the temperature fields respectively.

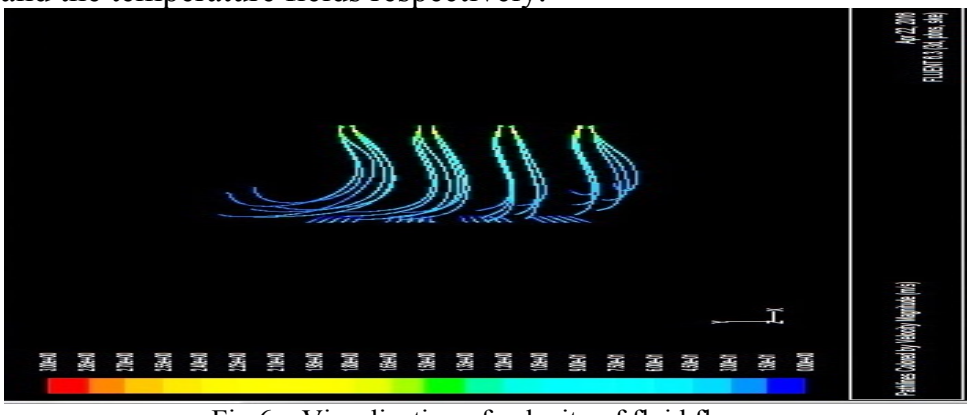

Fig.6 – Visualization of velocity of fluid flows

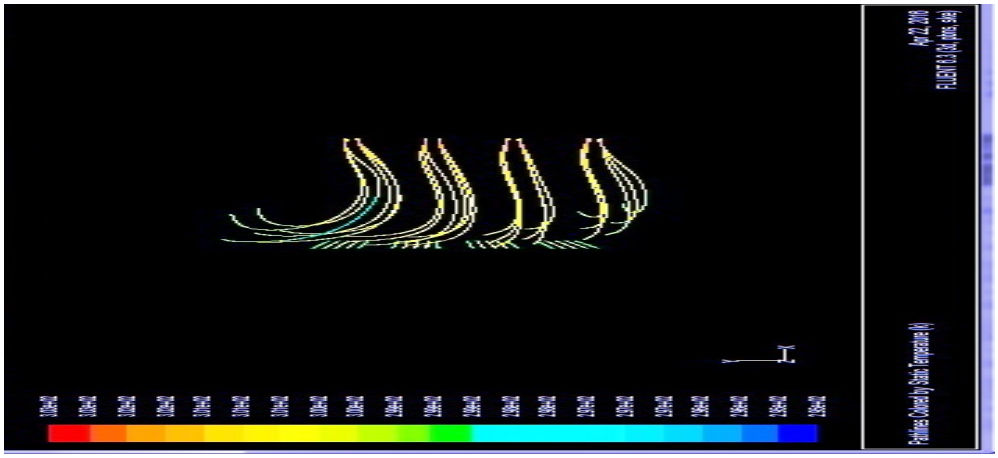

Fig.7 - Visualization of temperature of fluid flows

Fig.8 – Visualization of velocity vectors in the room

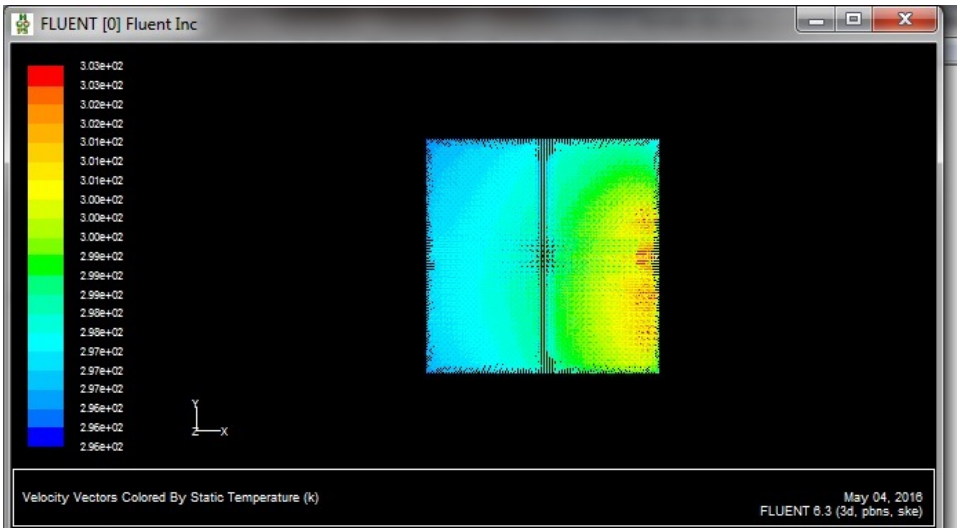


Fig.9 - Visualization of temperature vectors in the room

On fig. 6-7 are given the visualization of the velocity and temperature of the flow. On fig. 8-9 are given the visualization of velocity and temperature vectors in the room. The boundary conditions are the same use in Section 3.

**5. Conclusion**:

This paper discusses the numerical modeling of hazards in room with AB-rechargeable batteries. First is presented the mathematical model of the vertical non-isothermal two-phase flow and the complexity of the obtaining of solution for this two-phase turbulent flow. Second the numerical analysis of vertical non-isothermal stream modeling the flow in a confined space is given. Based on the previously presented analytical solution are shown. This paper finishes with a comparison analysis between the numerical solution (based on analytical model) and numerical simulation with Fluent software.

Based on the numerical simulations and the obtained numerical results it is shown that values of the speed and the temperature in both cases are close. This gives us reason to conclude that the resulting distribution model is correct and can be used to calculate the parameters of hazards in a room that can be of great benefit in practice.

## References

[1]Abramovich, Theory turbulentnyiy Strings, Moscow 1984

[2]Antonov IC, Applied Fluid Mechanics, Sofia 2010

[3]Daly, A. and P. Zannetti. 2007. *An Introduction to Air Pollution –Definitions, Classifications, and History., Oxford Press 2007*

*[4]Daniel Valero, Fuundamentals of air pollution , Fifth Edition, 2014*

[5]Nikolov K., R. Velichkova, H.Lien, I.Antonov, Modeling of movement and heat exchange at gaseous harmful in enviroment, Proceedings of FPEPM 2015, vol 2 pp33-38, ISSN1314-5371

[6]Renato Bernardini, Air pollution: Sources, Control and effects, Indoor+Built environment, 1996,pp184-186

[7]R. Velichkova, I. Antonov, K. Nikolov, K. Grozdanov, M. Uzunova, *Modelling of the occurrence of fire in closed cars garages, EFEA, 2016 \Belgrade, udner preview*

# Thermal evaluation of a perforated panel for solar collector model for air pre-heating

Mihai Mira[1], Cristiana V. Croitoru [1], Ilinca Nastase[1]

Technical University of Civil Engineering Bucharest, CAMBI Research Center,
Adresa Pache Protopopescu, 66, Bucharest, Romania
*E-mail: cristianaveronacroitoru@gmail.com*

**Abstract.** *Perforated solar windows pre-heat the fresh air introduced in the building when the air is forced to pass through this solar heated perforated facade. The type of solar collector in this case is a perforated window, which has two attributes: let the natural light in and heats the introduced fresh air. The Plexiglas sheets form a heated cavity, collecting the Sun's energy. An experimental campaign on an innovative solar window was performed in the laboratory of Building Services from Technical University of Civil Engineering Bucharest. The solar window with lobed perforations was analyzed against the one with round perforations and the results indicated that the systems can attain a high thermal performance.*

**Key words:** solar window; air heating; lobed perforation;

## 1. Introduction

Nowadays, humans use five times more energy than 50 years ago, considering the number of people, the urbanization of certain parts and a developing industry [1]. Estimates from the International Energy Agency, without further action to limit this consumption, it is expected to increase with 33% by 2040 worldwide, growth driven primarily by India, China, Africa, the Middle East and Southeast Asia[2].

The efficiency and energy prices also are major concerns nowadays. Therefore, economic and environmental research was accelerated towards innovative and clean technologies. All these energy consumptions, whether it's heating or cooling demand, can be translated in terms of $CO_2$ emissions [3-5].

In this context the use of renewable energies is an interesting solution for satisfying the two requests: indoor quality and energy efficiency. Among these renewable energies, the usage of solar passive systems is easy to implement and accessible in the zones with solar potential [6]. These systems can have a significant contribution to attain high envelope performances and in the same time to save energy either for winter heating or for summer cooling. The multitude of solutions for using thermal energy from the Sun has important advantages but also disadvantages that maintains the research in this area.

Ventilated windows are another solar thermal recovery device which seems to offer new possibilities of development in this domain. Indeed, in countries having a

cold climate during the winter, using a double window in building façades is a current practice. Transforming these double windows in passive air heating systems has the advantage of providing pre-heated air for winter ventilation which, otherwise, would enter the building at outdoor air temperature [7-9]. The air channel between the two windows is then used as a path to the ventilation air, further connected or not to another ventilation device (Fig. 1a).

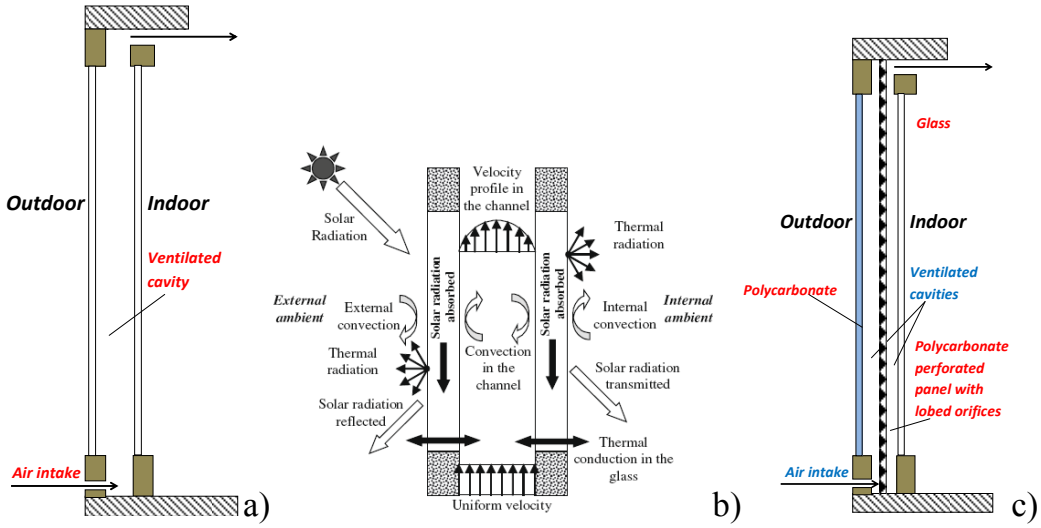


Fig. 1 Ventilated windows: a) schematic drawing of a simple ventilated window, b) layout of convective heat transfer in a ventilated window [10], c) innovative ventilated window

This air is pre-heated within the air channel between the windows by heat that is lost from the building and also by solar gains inside the window, before it is delivered inside warmer than it is outside. Part of the heat loss from inside through the window is returned back to the room by the air flow, acting as a heat recovery unit. Incident solar radiation upon the window warms its components being part of that heat removed by the air flow delivering it into the room, acting as a solar collector.

In their studies, Carlos et al. [7-9] putted an evidence a heat loss reduction up to 30% in the cases when a ventilating windows system is used compared to classical, non ventilated, double windows. In hot climates, if the heated air is evacuated in the exterior, the air flow from natural or forced convection (Fig. 1b) act as a protection screen improving thermal insulation of the window [10].

## 2. Methodology

As seen in Fig.1c, we propose a new type of perforated window which allows a better mixing between the heated air and the aspirated airflow from the exterior. The purpose of this article is to evaluate the thermal performance of such a setup and to compare the results between two types of perforations: round and lobed ones.

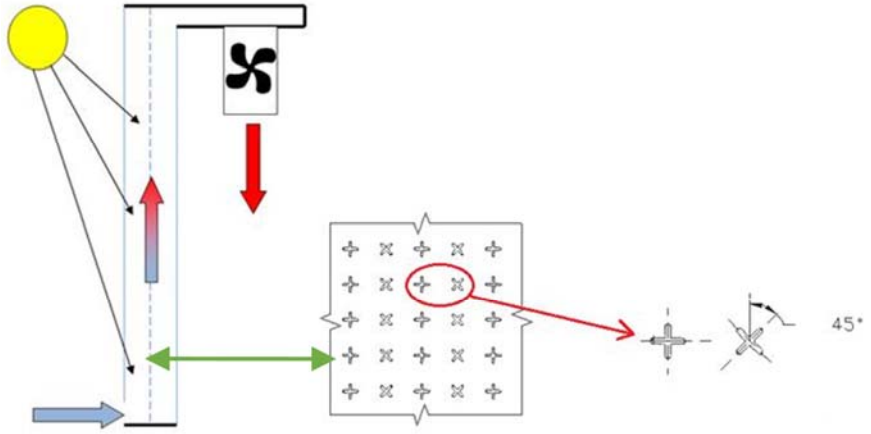


Fig. 2 Functional scheme of the experimental setup with the details of the lobed perforations on the Plexiglas sheet

The experimental campaign was performed inside a laboratory. The system is composed by two parts: the Plexiglas box with the perforated sheet inside and the exhausting system (Fig 3). The insulated box is attached through a circular pipe to an exhausting fan, forcing the air to pass through the window, fact which will accelerate the mixing between the interior air and the aspirated airflow. The airflow is varied with a direct current electrical source, obtaining values from 63 to 210 $m^3/h/m^2$.


Fig. 3 Experimental setup in the laboratory

The source of light was generated by six halide lamps of 500W each, which were simulating the sun radiation. The studies [11] indicate a radiation level of 800 $W/m^2$ so the lamps were evenly disposed to cover uniformly the metal plate.

The cases studied refer to classical circular and lobed perforation, as seen in Fig. 2. The equivalent diameter, $D_e$, of each perforation is 5 mm and the space between two orifices is $4D_e$. This lobed geometry, studied for innovative air inlets, has the advantage that for the same effective area (same equivalent diameter $D_e$) the perimeter of the lobed perforation is significantly larger than the circular one, while the airflow mixing is increased due to specific vortical structures in the air jet.

The airflow was determined by an Iris type damper for measuring airflows induced by the DC source to the fan. The mean velocity was integrated on the surface of the duct section, obtaining the airflow. Several thermocouples type K coupled to ALMENMO 2890-9 station were used to evaluate the temperature of heated air at the outlet and ambient air.

## 3. Results

The results indicated an interest in using this kind of air heating systems, with an increase in the temperature between 6.5 and 13°C for the two cases studied. The stabilization time was for all the points measured of about 17 min, as seen in Fig 4 a) and b) for the airflow of 63 $m^3/h/m^2$ or 30 $m^3/h$. Approximately the same conditions were obtained for the two studied cases, but the purpose of this investigation is to evaluate the air temperature increase between the ambient air and the air inside the box, near the extraction fan.

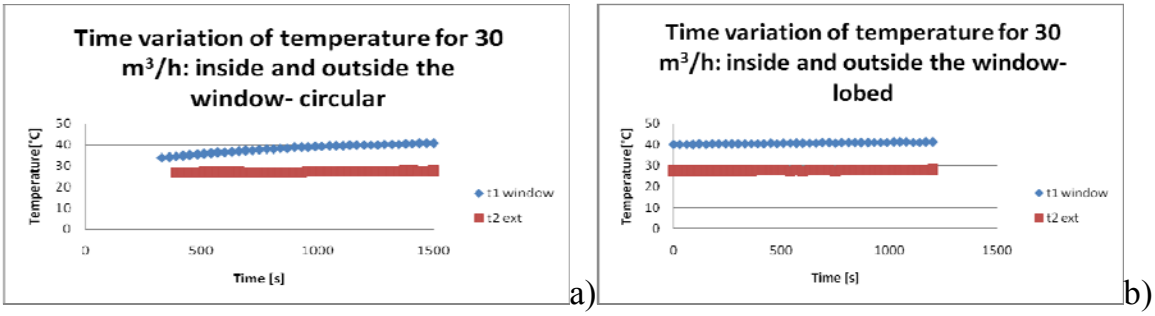


a) b)

Fig. 4 Temperature increase variation over the stabilisation period of approx. 17 min for the circular and lobed case

When comparing the temperature difference for all the points of measure, we can observe that this difference decreases with the increase of airflow value, starting for example with 12 °C for 63 $m^3/h/m^2$ and ending at 6 °C for 210 $m^3/h/m^2$, for the circular case.

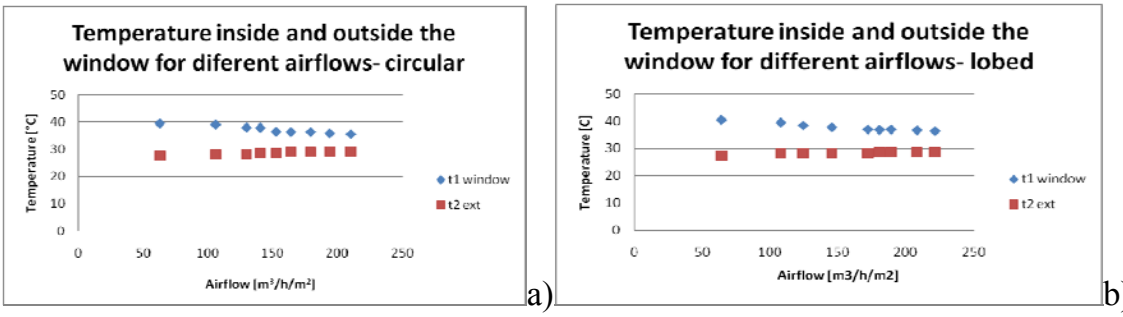


a) b)

Fig. 5 Temperature difference between heated air and ambeint air for the circular and lobed case when changing the airflow

The same tendency can be observed for the lobed case, with an increase in the measured temperature difference, especially for higher airflow values.

The projection of the temperature increase for the two cases studied can be better seen in Fig. 6, when comparing the results. The lobed perforations, with the advantage of the higher induced airflow rate, allows a better mixing between the ambient air and the air heated inside the cavity of the window. This kind of device, with perforated panel inside the window, has never been tested before considering the existing literature. The temperature rise between 6 and 13°C could be interesting for indoors which require lower temperature like industrial deposits.

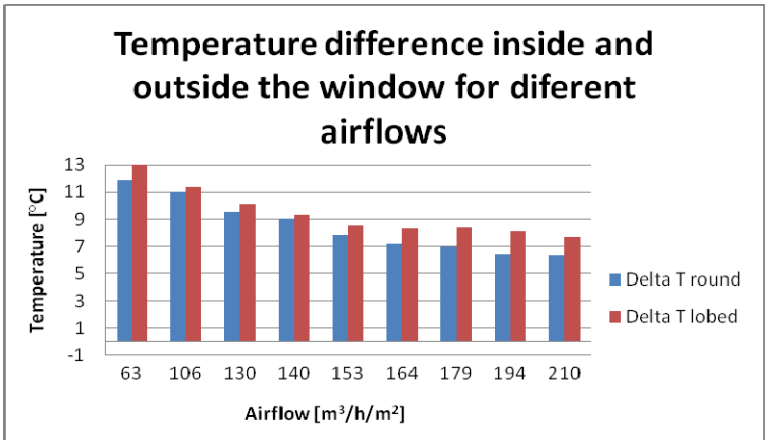


Fig. 6 Temperature difference between heated air and ambient air for the two cases studied

## 4. Conclusions

A new ventilated window system was tested in laboratory conditions. The perforated sheet inside the window allows a better mixing between the aspired air and the air heated but the radiation between the external sheets. The temperature rise, of maximum 13°C can be attained for the lobed case, for 63 $m^3/h/m^2$. The study needs further investigations, considering the materials used, perforations type and to integrate the temperature rise into the global energy efficiency of the system

## Acknowledgment

This work was supported by Grant of the Romanian National Authority for Scientific Research, CNCS, UEFISCDI, PN-II-PT-PCCA-2011-3.2-1212.

## References

[1] J. Fenger, Air pollution in the last 50 years – From local to global, Atmospheric Environment, 43 (2009) 13-22.
[2] IEA, World Energy Outlook 2015, in: W.E. Outlook (Ed.), Internationl Energy Agency, 2015.
[3] IEA, Renewables for heating and cooling: untapped potential. France: OECD/IEA;, in, 2007.
[4] IEA, World energy outlook 2007: China and India insights. France: OECD/IEA;, (2007).
[5] IEA, Worldwide trends in energy use and efficiency: key insights from IEA indicator analysis. France: OECD/IEA, in, 2008.

[6] IEA, Solar's Untapped Potential, in, 2005.
[7] J.S. Carlos, H. Corvacho, P.D. Silva, J.P. Castro-Gomes, Real climate experimental study of two double window systems with preheating of ventilation air, Energy and Buildings, 42 (2010) 928-934.
[8] J.S. Carlos, H. Corvacho, P.D. Silva, J.P. Castro-Gomes, Modelling and simulation of a ventilated double window, Applied Thermal Engineering, 31 (2011) 93-102.
[9] J.S. Carlos, H. Corvacho, P.D. Silva, J.P. Castro-Gomes, Heat recovery versus solar collection in a ventilated double window, Applied Thermal Engineering, 37 (2012) 258-266.
[10] K.A.R. Ismail, C.T. Salinas, J.R. Henriquez, A comparative study of naturally ventilated and gas filled windows for hot climates, Energy Conversion and Management, 50 (2009) 1691-1703.
[11] M.A. Leon, S. Kumar, Mathematical modeling and thermal performance analysis of unglazed transpired solar collectors, Solar Energy, 81 (2007) 62-75.

# Advanced thermal manikin with neuro-fuzzy control

Mircea Dan[1], Paul Danca[2], Ioan Ursu[1], Ilinca Nastase[2],

[1]INCAS - National Institute for Aerospace Research "Elie Carafoli"
B-dul Iuliu Maniu 220, Bucharest 061136, Romania
*E-mail: ursu.ioan@incas.ro*

[2] CAMBI, Technical University of Civil Engineering in Bucharest, Building Services Department, 66 Avenue Pache Protopopesc; 020396, Bucharest, Romania

**Abstract.** *This paper is presenting one among the five prototypes of thermal manikins conceived at the Building Services Faculty (Thermal-Hydraulic Systems Laboratory) at the Technical University of Civil Engineering of Bucharest and developed by the National Institute of Aerospace Research Elie Carafoli in the framework of the project EQUATOR. This particular prototype has an advanced anatomic shape, with 79 independent active zones, temperature sensors and its own in-house software for data acquisition and control of the zone's surface temperature. The paper is presenting the all stages needed for the development of an advanced thermal manikin with neuro-fuzzy control for research purposes. All composing parts of the manikin and the validation strategy were presented.*

**Key words:** advanced thermal manikin, thermal confort, neuro-fuzzy control

## 1. Introduction

Thermal comfort is a complicated concept defined by a plurality of subjective parameters. A thermal manikin is a human model designed for testing of thermal environments without some inconveniences inherent in human subject testing. Thermal manikins are mainly used in automotive, indoor environment, outdoor environment, military and clothing research. Thermal manikins have a long time history, being used for more than 70 years. At the beginning they were used for testing clothing for soldiers by the US Army [1]. The shape and heating system were very simple at that stage. Nowadays the shape and complexity of the available thermal manikins raised and start to approach the complexity of the human body. The number of independently controlled zones increased from a single zone corresponding to the entire surface up to 120 individually controlled zones [2]. The material used for developing the thermal manikin have diversified, from copper to plastic and carbon fiber to skin like silicone. Most of them try to simulate the human body and the associated heat emission in the environment, while others are more or less complex measurement devices for assessing thermal environment quality by simulating the human body thermal regulatory mechanisms and measuring its heat loss towards its environment [1]. The most advanced of them can also simulate body sweating and heat exchange through evaporation [1-4]. This paper is presenting one advanced thermal

manikin with neuro-fuzzy control that was developed in the framework of the EQUATOR project [5].

| **Nomenclature** | |
|---|---|
| $\theta$ [m] | temperature |
| $P$[W] | mean power consumption calculated using a sliding average over a preset period of time |
| $S$ [m²] | surface area of manikin's region |
| *Subscripts* | |
| ech | equivalent |
| reg | region |

## 2. Manufacturing the heating part of the manikin

This particular prototype, is a female manikin, familiarly called Suzi. It has an advanced anatomic shape, with 79 independent active zones, 5 temperature sensors for each zone and its own in-house software for data acquisition and control. The thermal manikin was designed for both seated and standing postures. The size of the manikin is a standard human size with a total surface of 1.8m² (Fig. 1a). The base structure of the manikin is made of polyvinyl. The surface of the manikin has been covered with a 5mm insulation layer (Fig. 1b).

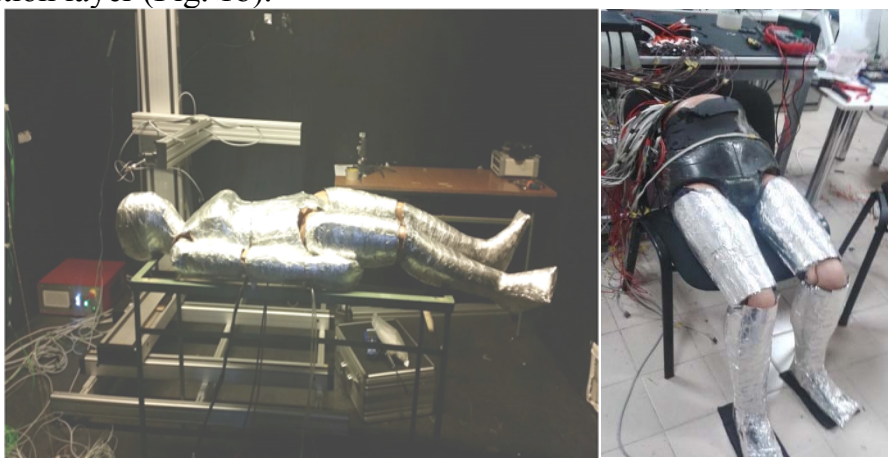

Fig.1 a) Thermal manikin simulating a patient, b) manufacturing the body parts – the black part is representing the insulation layer

The heating solution chosen for this prototype consist in using five types of elementary patches (Fig. 2a) that are combined to cover each individually controlled zone. The patches are made of a thin layer of silicone (1.5mm) that includes a heating circuit made of nickel chrome heating wire and etching foil. The heating silicone patches are presented in Fig. 2b. Several solutions of films and heating materials were tested but the heating silicone patches were found to provide the best uniformity in terms of temperature distribution. In Fig. 4 are compared the surface temperature distributions of a flexible polyamide heating film, of a silicone patch and of the human

skin of the hand. The heating film patches were placed on the insulation layer on the polyvinyl base using with double side adhesive tape. After covering a body zone the electrical connections and circuits were created. Every electrical connection was tested for leakage for safety reasons. The electrical wire was embedded inside the manikin (Fig 1b). In order to ensure that the thermal load of the film mounted over the wires is not influencing the cable stability we selected special electrical wire that works at temperatures above 7°C. During a preliminary test, without any control of the circuits, the temperature of each zone stabilized at 45°C when the room temperature was stable at 24 °C, a rather encouraging result offering a wide range to control the temperature of each zone and the possibility to simulate different cases of body heat release.

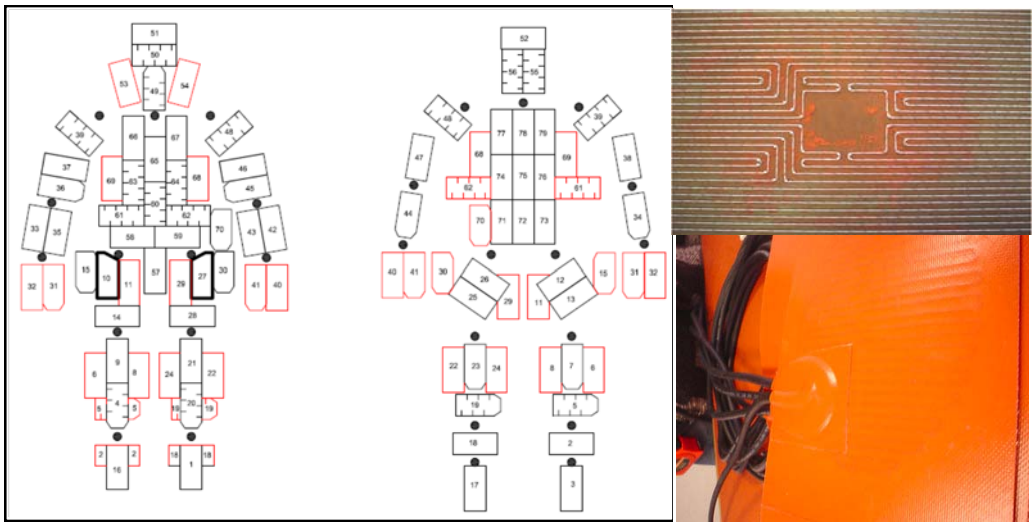

Fig.2 a) Distribution of the anatomic zones individually controlled (red patches are corresponding to the other side), b) Photographs of the heating silicon parts that are composing the zones

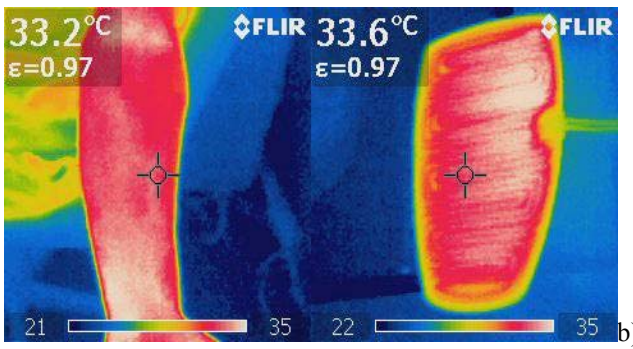


b)

Fig. 3 ) Comparison between the surface temperature distribution of a silicone patch and the human skin of the hand [6].

Even if this type of heating element appeared to be the best possible solution for the current project there are still some regions were the heating circuit is not present creating zones were the temperature values are lower (i.e. the borders of each patch – see Fig. 6 b for instance). As a non-uniform temperature of the manikin surface has to be avoided [7] we decide to cover the entire manikin surface with adhesive aluminium foil to ensure enhanced conduction heat transfer. Finally, in order to facilitate further investigations with a thermal (IR) camera the entire manikin surface was covered with

a transparent adhesive film. In order to validate the heating part of the manikin prototype we performed several tests, concerning the distribution of the surface temperature of each manikin, the sensors employed for the control part, the electrical characteristics of the used components.

For the control part of the surface temperature of the manikin we choose digital sensors given the adopted strategy presented previously. The sensors are the model TSic T501 manufactured by IST. Each sensor was carefully tested. In Fig. 5 a) and b) are presented examples of response at thermal solicitations over time for eight of these sensors with and without calibration. During the calibration process we used a thermostatic water bath Lauda Eco with immersion thermostat Lauda Eco Silver (Fig. 12 c).

Fig 4. a) TSic T501 sensors used for the measurement and control part of the thermal manikin , b) thermostatic water bath Lauda Eco with immersion thermostat Lauda Eco Silver

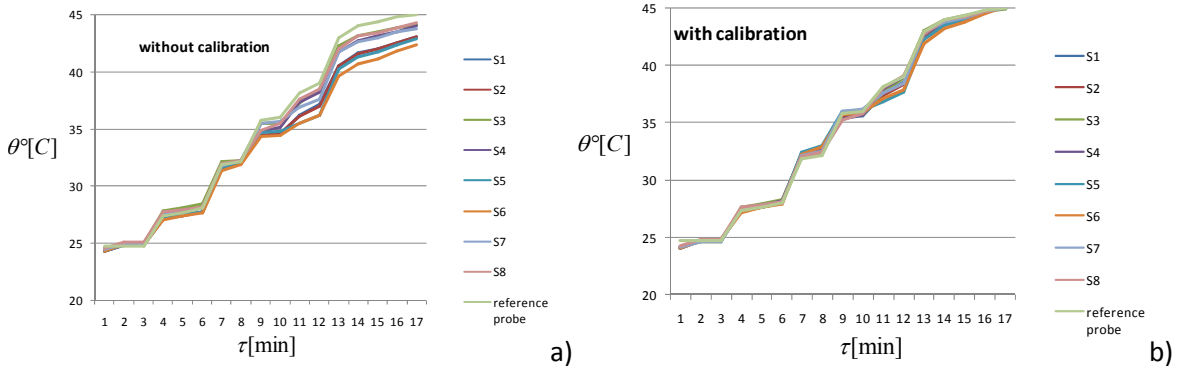


Fig 5. Response at thermal solicitations over time of TSic TO92 sensors: a) without calibration, b) with calibration

## 3. Architecture of the control system of the thermal manikin

The thermostatic manikin system consists of 79 patches each with a heating element (24 Ohms constant resistance) and 5 analog temperature sensors (TSic 501) mounted on each patch surface used by the control system to maintain a constant preset temperature of the manikin surface. The 395 acquisition channels are collected by the multiplexer interface (Fig. 6) to help miniaturizing of the electronic system, by reducing the space occupied by wires, thus being able to fit inside the manikin.

For the development of the system there were used two boards from National Instruments (myRIO 1900 and sbRIO 9363). Both have a unit of sequent calculus

(x86) and unit of matrix calculus. To connect the temperature sensors to the development board there was used a multiplexer interface based on HEF4067B. The control of the MOS transistors used for the execution system was achieved through an interface made of SN7407 circuits. Basic architecture of the maniquin system is given in Fig. 7.

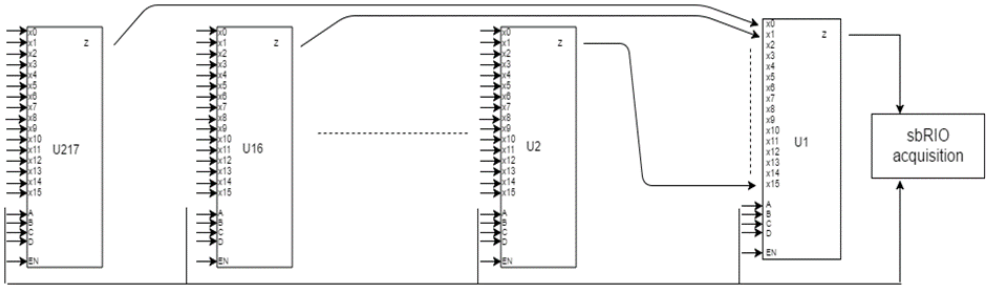


Fig 6. Multiplexer simplified circuit diagram

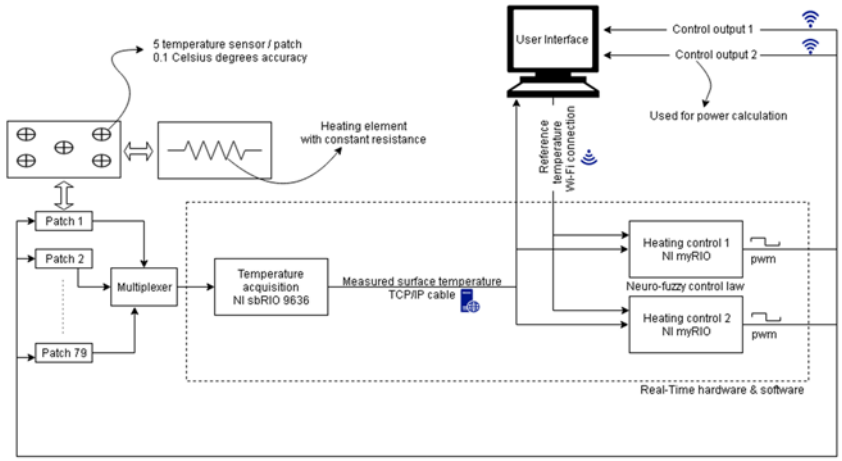


Fig. 7. Basic architecture of manikin system

The FPGA software on the sbRIO 9636 handles the acquisition of data from the multiplexer interface which, instead of requesting one input at a time, collects all the inputs and separates them by shifting the register in the temperature data memory. The software from myRIO 1900's FPGA creates the PWM pulse used to control the patch surface. Both NI boards have implemented real-time software, the acquisition device also processes the data to obtain reliable mean temperature of every patch using a fault detection and isolation algorithm, while de heating control devices, using the data processed by the acquisition board, generate robust and adequate signal using the neuro-fuzzy controller. The real-time hardware and software can run independently from the computer user interface, with the limitation of maintaining the last (or default) requested set point of temperature.

The computer software allows the user to load set points for several testing situations, change the set point on each patch independently and monitor the behavior of the temperature data and control system. The user can also view the average equivalent temperature displayed graphically on a simplified model of manikin and average power consumption.

The necessity of processing a high amount of information (395 acquisition channels, signal filtering, etc.) and generating proper signals for 79 command channels, as well as the strict timing, provided by the NI boards Real-Time processor and required for the control of electronic circuits (multiplexer and MOS driver interface), lead clearly to the conclusion that this technology is the best solution for the maniquin system. The control algorithm for the command channels was converted into software for the sequent calculus unit of the NI boards.

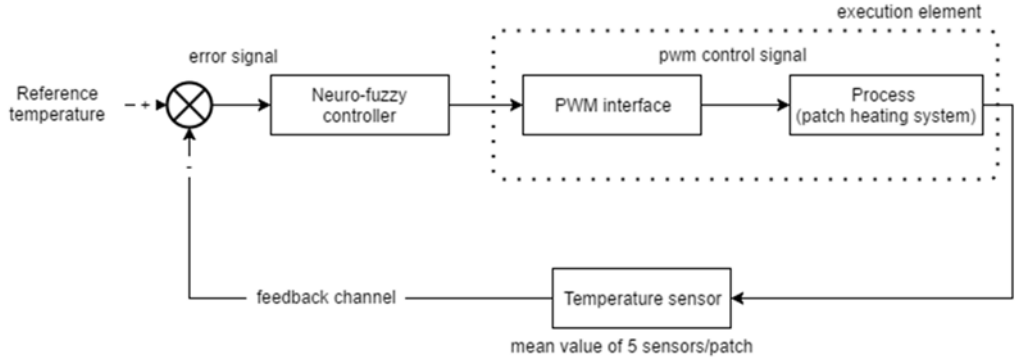


Fig 8. Control system diagram for one control channel

Block-schema for the control of one channel is shown in Fig. 8. PWM (pulse width modulation) is a well known technique to produce analog signal using digital devices that output a square signal by switching on and off the output port. By modifying the period that the signal is on and off, a voltage between 0 and 24V (the maximum voltage recommended for the patches) can be provided. Since myRIO 1900 boards can output only 3.3V in DIO (digital I/O) ports, there has been added an interface to convert 3.3V TTL signal to 5V CMOS signal needed by the transistors to open and close the 24V supply circuit according to the PWM control generated by the neuro-fuzzy controller. In fact, the salient feature of neurocontrol and fuzzy logic control, which distinguish them from the traditional control and adaptive approaches, is that they provide a model-free description of the control system. Thus, a lot of troubles relating to the robustness of the system can be surpassed. Both neural networks and fuzzy logic show great potential for controlling systems that are difficult or impossible to model using traditional techniques. The advantages of neural networks are twofold: learning ability (a neural network mimics the function of the brain) and versatile mapping capabilities from input to output (certain types of neural networks are universal approximators giving so special abilities in adaptive control and system identification). In its turn, the fuzzy set theory provides a suitable tool for both the treatment of intrinsic inexactness of the description in a dialectical context and imitation of human thinking in the process of compromise in making a decision [8], [9]. For the thermal manikin, the temperature is optimally controlled: neural network minimizes the temperature reference tracking error. For the synthesis of neuro-fuzzy control, only a measured temperature information is required, and it is not necessary to know a mathematical model of the manikin system!

## 4. Thermal comfort indicators

The equivalent temperature that represents an indication of thermal comfort is obtained by evaluating the power consumption of a region of the manikin. Due to the pwm control signal which commutes on and off between maximum and minimum voltage, the power consumed by the thermostatic system was calculated by creating a calibration slope between pwm duty-cycle and the power calculated as a point by point mean of a single pulse period. The voltage drop on the patch was calculated differentially by measuring with the Hantek DSO5102P oscilloscope the voltage drop on the whole circuit from which it was subtracted the voltage drop on the transistors. The current consumed by the patch was measured with TH5A current transducer.

$$\theta_{ech} = \theta_{reg} - \frac{P}{S \cdot h_{cal}} \tag{11}$$

where $\theta_{ech}$ = equivalent temperature; $\theta_{reg}$ = mean temperature of surface region calculated using a sliding average over a preset period of time; S = surface area of manikin's region; P = mean power consumption calculated using a sliding average over a preset period of time; $h_{cal}$ = convection coefficient calculated with equation (1) at constant environment temperature ($\theta_{ech}$) of 24 ºC and manikin's surface temperature controlled at 34 ºC. Experiments revealed that by modifying the environment temperature from 20 to 40ºC the changes in power consumption were indistinguishable (Fig. 9).

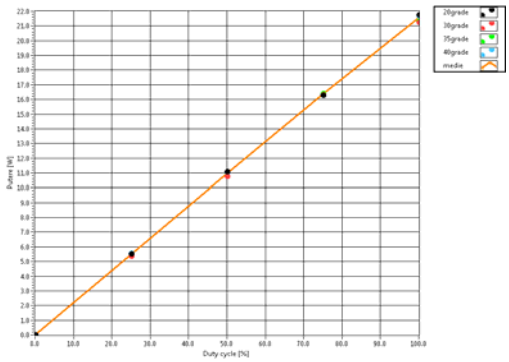

Fig 9. Power variation as function of PWM duty-cycle

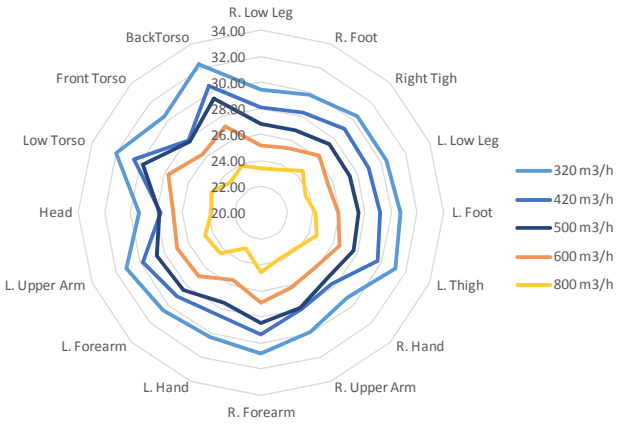


Fig. 10. Example of $\theta_{ech}$ distributions obtained from the thermal manikin data for several air flows

Compared to classical measurement systems which give the possibility of estimating the global PMV, the thermal manikin gives the advantage of assessing locally a predicted local sensation, either through the equivalent temperature either through a derived local PMV. The thermal manikin represents a worthy tool for the thermal comfort analysis in laboratory configurations and in real field case studies being a method of investigating local discomfort trough the local distributions of the equivalent temperature of the segments of the manikin. This kind of representation allows, for instance, the inspection of the uniformity of an environment. In Figure 10, we show an example of equivalent temperature distributions for several air flows defined by Nilsson [10] or in the standard EN ISO 14505/2 [11] for a studied air grille for operating rooms.

## 6. Conclusions

This paper is presenting the all stages needed for the development of an advanced thermal manikin for research purposes. All composing parts of the manikin and the validation strategy were presented. A carefully check-up of all components was necessary and some of the tests we done were time consuming. The model is fully functional and the temperatures of each body zone can be easily modified in accordance to our needs.

## Acknowledgements

This work was supported by the grants of the Romanian National Authority for Scientific Research, CNCS – UEFISCDI, project numbers: PN-II-ID-PCE-2011-3-0835 and PN-II-PT-PCCA-2011-3.2-1212".

## References

1. Holmér, I., *Thermal manikin history and applications.* European Journal of Applied Physiology, 2004. **92** p. 614-618.
2. Jambunathan, K., et al., *A review of heat transfer data for single circular jet impingement.* International Journal of Heat and Fluid Flow, 1992. **13**: p. 106-115.
3. Alahmer, A., et al., *Vehicular thermal comfort models; a comprehensive review.* Applied Thermal Engineering, 2011. **31**(6–7): p. 995-1002.
4. Sakoi, T., et al., *Thermal comfort, skin temperature distribution, and sensible heat loss distribution in the sitting posture in various asymmetric radiant fields.* Building and Environment, 2007. **42**(12): p. 3984-3999.
5. *EQUATOR: Advanced strategies for high performance indoor Environmental quality in Operating Rooms - PN-II-PT-PCCA-2011-3.2-0512*. 2012-2016, UEFISCDI.
6. Dogeanu, A., *Cercetari privind realizarea unor proceduri performante de evaluare si clasificare a microclimatului interior, Teza de doctorat*. 2015.
7. Gardon, R. and J.C. Akfirat, *The role of turbulence in determining the heat-transfer characteristics of impinging jets.* International Journal of Heat and Mass Transfer, 1965. **8**: p. 1261-1272.

8. Ursu, I., et al., *Neuro-fuzzy synthesis of flight controls electrohydraulic servo*. Aircraft Eng. and Aerospace Technology, 2001, **73**, pp. 465-471.
9. Ursu, I., et al., *Switching neuro-fuzzy control with antisaturating logic. Experimental results for hydrostatic servoactuators*, Proceedings of the Romanian Academy, Series A, Mathematics, Physics, Technical Sciences, Information Science, 2011, **12**, 3, 231-238.
10. Nilsson, H., et al. *Equivalent temperature and thermal sensation - Comparison with subjective responses*. in *Comfort in the automotive industry- Recent development and achievements*. 1997. Bologna, Italy.
11. ISO, *Ergonomics of the thermal environment -Evaluation of thermal environments in vehicles Part 2: Determination of Equivalent Temperature*, in *ISO 14505-2:2006*. 2006, ISO.

# Climatizarea la un Dispecerat al serviciilor spitalicesti din Statul Maine – SUA

## Air Conditioning at a Hospital Dispatch Center in the State of Maine – USA

Ing. Ilina Matei Traian – Ilina Engineering PA – Statul Maine – SUA
Dr.ing. Ilina Mihai – Prof. Universitar, UTCB FII, București, România

**Rezumat**
Cladirea prezinta unele particularitati legate de activitatea desfasurata in spatiile de lucru. Instalatiile de incalzire ale incaperilor s-au realizat cu doua sisteme: incalzire cu aer cald in toate incaperile in perioada rece cu temperaturi exterioare in limitele temperaturii de calcul si cu corpuri statice in perioadele cu temperaturi mai scazute, considerata ca sursa de adaos. Sistemul de incalzire cu corpuri statice asigura si incalzirea de garda in perioada de inactivitate. O noutate in sistemul de incalzire cu aer cald prin introducerea unor unitati SDV pe canalele de distributie aer cu rolul de a compensa instantaneu modificarile de presiune ale aerului care pot produce cresterea sau scaderea debitelor in punctele terminale. De subliniat si solutia adoptata pentru sursa termica unde prepararea aegentului termic se face in doua cazane de apa calda cu combustibil solid ( peleti) si o instalatie speciala de depozitare si alimentare a cazanelor complet automatizata.

cuvinte cheie: încălzire cu aer cald, încălzire cu corpuri statice

**Abstract**
In this article is described the HVAC systems for a medical office building. Heating system in the building is primary hot air that is maintaining the zone or room temperature at the setting point for the outdoor design temperature and with secondary perimeter hydraulic heaters engaged when outdoor temperature is below the design parameters. The perimeter hydraulic heating system is used on night setback or un-occupied periods when the primary hot air system is off. The novelty of this particular system represents the VAV boxes with re-heat hot water coils installed in the ductwork that modulates the air volume for the designated ventilation zone to maintain the zone or room set-point. These units are used in the same manner to maintain the setting point for cooling as well the hot water for the heating system is generated by two pellet boilers and one LP gas boiler. The pellets delivery and storage system is completely automatic.

key-words: hot air heating, hydraulic heating

**Cladirea** are doua niveluri cu structura de rezistenta din lemn si fundatia din beton armat. Peretii exterioori sunt de tip sandwich, izolati termic avand rezistenta termica R = 4 - 5 $m^2$.K/W, Spatiile din interior sunt despartite cu pereti tot din lemn, izolati termic si fonic si captusiti cu placi din rigips. A fost data in exploatare in anul 2015.

Fig. 1. Cladirea

**Instalatia de incalzire.** In functie de activitatea desfasurata s-a adoptat sistemul de incalzire cu aer cald si corpuri de incalzire statice

- *solutia de incalzire cu aer cald* s-a utilizat in toate incaperile din cladire in perioada cu activitate continua. Tinand seama de tipul camerelor, importanta lor, activitatea desfasurata, climatul din interior, si pozitia lor in raport cu orientarea, s-a impartit spatiul din cladire in patru zone, fiecare zona fiind prevazuta cu o centrala de tratare a aerului cald, de la care prin retele de canale s-a facut distributia aerului cald la terminale.

- Centrala de tratare a aerului cald, fig.2, cuprinde elementele de baza: camera de amestec aer cald din incaperi cu aer rece din exterior, filtru de aer, bateriile de incalzire si racire precum si un ventilator centrifugal. In plus centrala de tratare este dotata si cu aparat de reglare debit de aer proaspat in perioada rece. El este montat langa camera de tratare pe canalul aerului rece si este executat dintr-o carcasa metalica in interiorul careia se gaseste o clapeta mobila actionata de un motor electric. Rolul aparatului este de a regla debitul de aer rece necesar realizarii conditiilor de confort fiziologic din incaperi. Clapeta prezinta trei pozitii (fig a- cu trecerea intregului debit de aer rece prin canal, b- cu inchiderea circulatiei aerului rece prin canal, c-cu pozitie variabila, in functie de temparatura exterioara, asigurand debitul de aer proaspat necesar conditiilor fiziologice. In situatiile extreme, cand temperatura exterioara scade sub valoarea luata in calculul debitului de aer proaspat, clapeta se pozitioneaza astfel incat sa se asigure un debit minimum de 10 % din cel necesar.

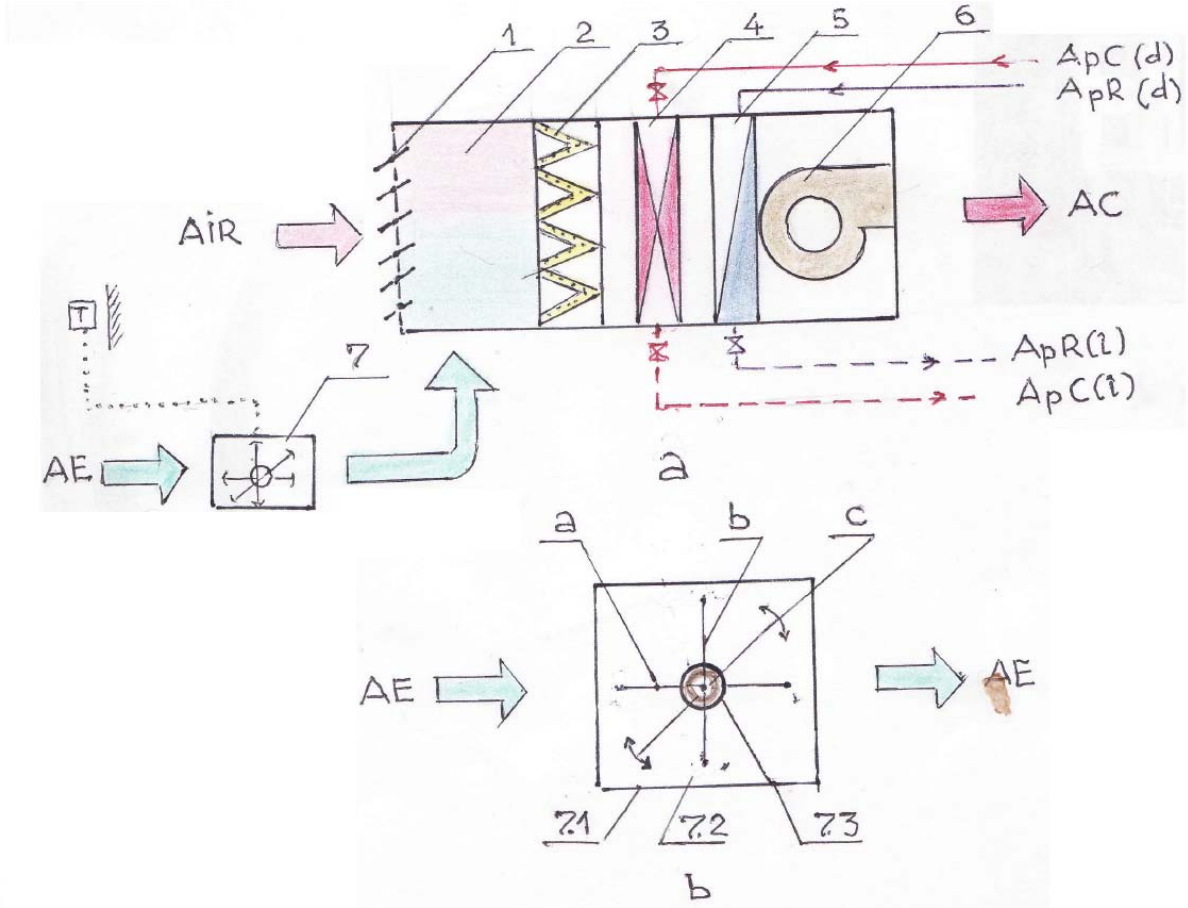


Fig. 2 Camera de tratare aer cald
a- schema camerei de tratare b- shema de principiu a aparatului de reglare debit de aer
1-jaluzele reglabile; 2- camera de amestec, 3- filtru de aer, 4- baterie de incalzire, 5- baterie de racire, 6 ventilator centrifugal, 7 – aparat de reglare debit de aer exterior, 7.1 - carcasa metaica, 7.2 - clapeta , 7.3 - motor electric. AE - aer exterior, AIR- aer cald din interior. AC -aer cald; ApC(d) si ApC(r) agent termic apa calda ducere /intoarcere; ApR(d) si ApR(r) apa racita ducere/intoarcere

- R e t e a u a d e c a n a l e d e d i s t r i b u t i e care leaga camerele de tratare cu terminalele (spatiile de lucru). Este executata din tabla de inox izolata termic si acoperita cu folie de aluminiu. In punctele cu ramificatii sunt prevazute clapete actionate manual. In zona consumatorilor, acestea sunt grupati in functie de debitele de aer solicitate, debite ce variaza in functie de desfasurarea activitatii in spatiul incaperilor. Pentru asigurarea unei bune repartizari a debitelor de aer cald, in capetele retelei de distributie din zona respeciva sunt prevazute unitati terminale tip SDVcu comenzi digitale, montate pe canalele de aer fig 3. Au rolul de a controla debitul de aer introdus in incaperi sub actiunea unui termostat ( montat intr-una din camere). Asigura o buna repartizare a debitelor de aer in functie de necesitati, economisind si energia realizarii aerului cald. Prin acesta monitorizare compenseaza instantaneu modificarile de presiune ale aerului ce pot duce la cresterea sau scaderea debitului de aer cald.

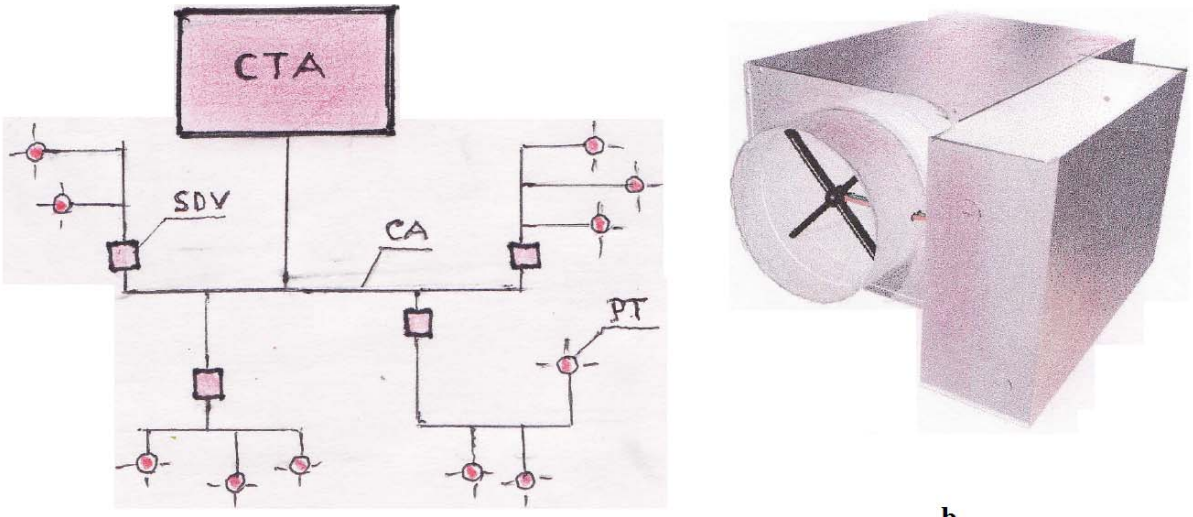


Fig. 3 Distributia aerului cald
a- schema instalatiei de distributie a aerului cald, b- aparatul SDV – aparat de control al debitului de aer in canal ; CTA- camera de tratare aer cald cu comanda digitala; CA – canal de aer.
PT – puncte terminale

- *solutia de incalzire cu corpuri statice* realizata cu convectoare de plinta, amplasate in general in incaperile cu peretii exteriori si in grupurile sanitare. Aceste corpuri de incalzire asigura pe de o parte caldura necesara in incaperi in perioada in care sistemul de incalzire cu aer cald nu asigura temperatura de confort ( perioada cu temperaturi exterioare sub cea de calcul ) functionand ca sursa de adaos, iar pe de alta parte asigura si caldura necesara de conservare in incaperi in perioada de inactivitate in cladire (temperatura de garda).

**Sursa termica** amplasata in incinta cladirii, la parter, cuprinde utilajele si aparatura necesara producerii de apa calda pentru instalatiile incalzire si de preparat apa calda de consum (fig 4). Prepararea agentului termic ( apa calda 80/60 $^0$C ) se face in doua cazane cu peleti tip OkoFEN –Austria cu debite de caldura $\Phi_{cz}$ = 60 kW cu randamentul $\eta$ = 83,9 % si un cazan tip Wiessmann cu un debit de caldura $\Phi$ =60 kW ( considerat cazan de rezerva ) utilizand combustibil GPL. Combustibilul solid, peletii, este depozitat intr-o incapere adiacenta centralei termice. Cantitatea de peleti depozitata este de 9 tone. Atat modul de depozitare al peletilor cat si modul de alimentare cu peletii a cazanelor se face automat. Peletii sunt adusi in cinsterne speciale care sunt prevazute cu aparatura necesara descarcarii in depozit. ( pornirea si descarcarea peletilor se face automat). Alimentarea cazanelor cu peleti se face cu un agregat special care transporta peletii din depozit la cazane printr-o conducta din material plastic. Pornirea si oprirea alimentarii se face de aemenea automat fig.5. Aerul de combustie este in regim deschis cu o priza de aer in peretele exterior sursei termice si este adus la cazane de asemenea printr-o conducta din material plastic.

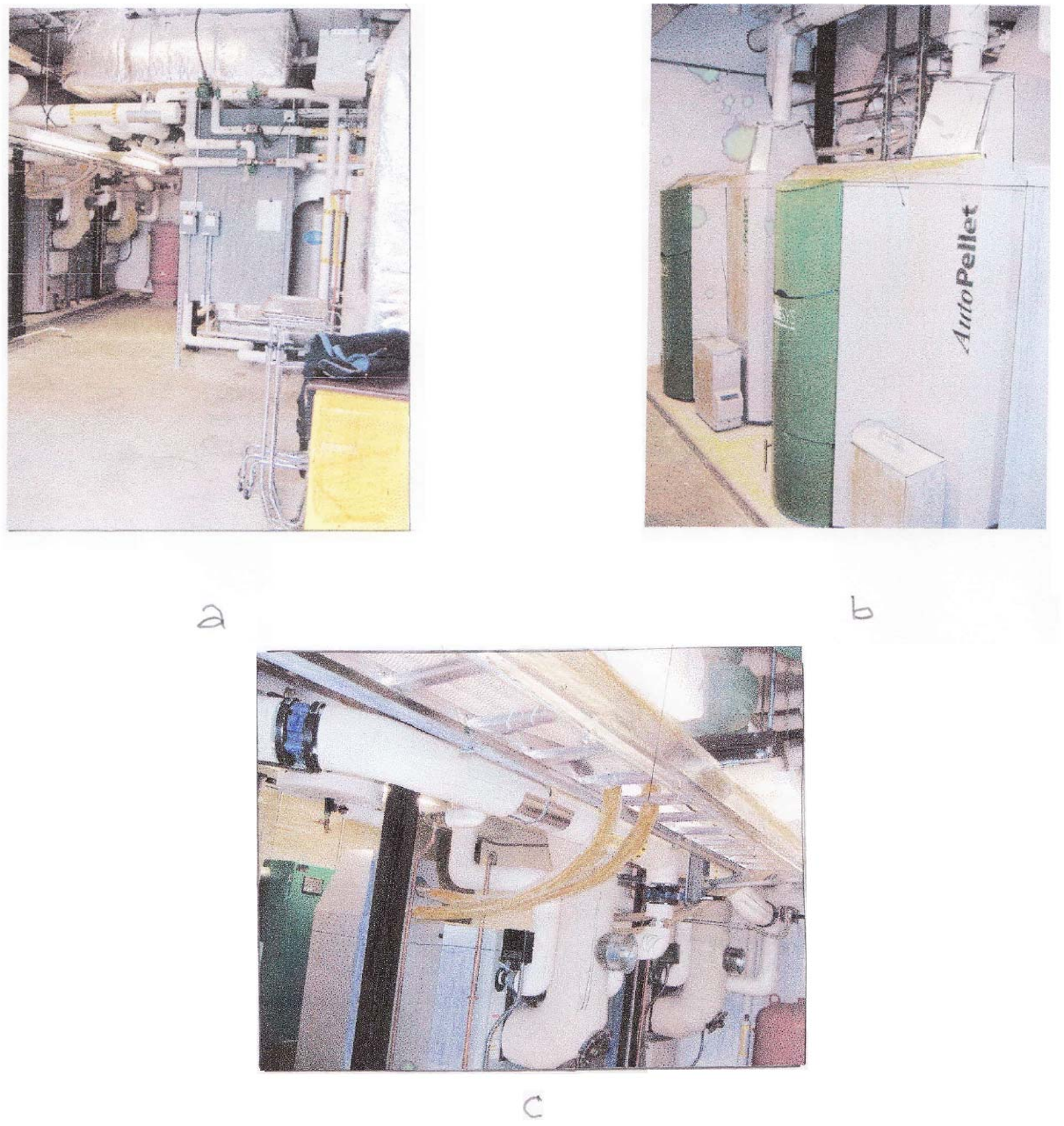


Fig. 4 Sursa termica
a-vedere de ansamblu a sursei termice, b- cazane tip OkoFEN –Austria, c- rcordurile de conducte din spatele cazanelor

**Climatizarea** s-a realizat tot cu aer, utilizand aceeasi camera de tratare, unde se prepara aer la parametrii necesari asigurarii conditiilor de confort in perioada calda. Apa racita s-a realizat intr-un chiller (statie cu pompa de caldura aer –apa exterioara) amplasata in apropierea cladirii fig 6.

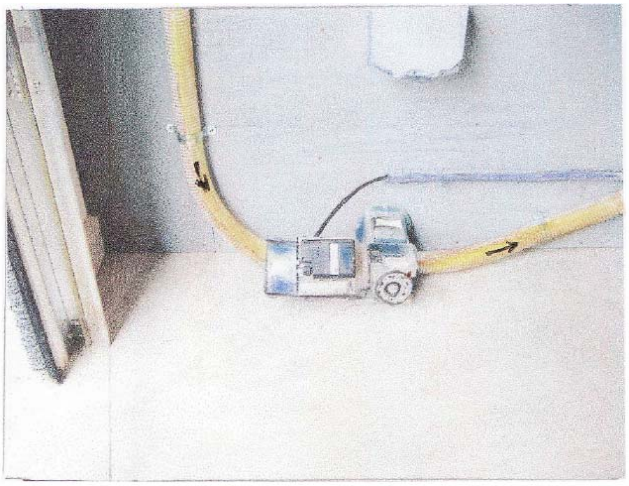

Fig. 5. Agregat de transport peleti

Fig. 6 Chiller

## Bibliografie

Patten Medical Office project – Design by Matei Ilina at ABM Mechanical, Bangor – State of Maine
ASHRAE Standard 90.1 – 2010 Edition
ASHRAE Standard 55 – 2010 Edition
ASHRAE Standard 62 – 2010 Edition
SMACNA – 2014 Edition

**REVISTA ROMÂNĂ DE INGINERIE CIVILĂ INCLUDE ARTICOLE DIN URMĂTOARELE DOMENII**

**ROMANIAN JOURNAL OF CIVIL ENGINEERING INCLUDE ARTICLES FROM THE FOLLOWING AREAS**

| | |
|---|---|
| . Mecanica structurilor | . Mechanics of structures |
| . Inginerie seismică și siguranța construcțiilor | . Seismic engineering and construction safety |
| . Inginerie urbană și dezvoltare regională | . Urban engineering and regional development |
| . Construcții civile | . Civil buildings |
| . Căi de comunicații, poduri și tunele | . Communication ways, bridges and tunnels |
| . Căi ferate | . Railways |
| . Drumuri și aeroporturi | . Roads and airports |
| . Construcții din beton armat | . Reinforced concrete buildings |
| . Construcții metalice | . Metal constructions |
| . Geotehnică și fundații | . Geotechnics and foundations |
| . Alimentări cu apă și canalizare | . Water supply and sanitation |
| . Tratarea apei | . Water treatment |
| . Epurarea apelor uzate | . Wastewater treatment |
| . Construcții hidrotehnice | . Hydro construction |
| . Îmbunătățiri funciare | . Land improvements |
| . Hidraulică și mecanica fluidelor | . Hydraulics and Fluid Mechanics |
| . Hidrologie, hidrogeologie și gospodărirea apelor | . Hydrology, hydrogeology and water management |
| . Protecția mediului în inginerie civilă | . Environmental protection in civil engineering |
| . Instalații pentru construcții | . Building services |
| . Management în construcții | . Construction Management |
| . Calitatea mediului interior | . Indoor environmental quality |
| . Acustica clădirilor și a instalațiilor | . Acoustic of buildings and installations |
| . Energetica clădirilor și instalațiilor | . Energy of buildings and installations |
| . Geodezie, fotogrammetrie, cartografie | . Geodesy, photogrammetry, cartography |
| . Termotehnică | . Thermotechnics |
| . Mașini și utilaje pentru construcții | . Constructions machinery |
| . Mecanică tehnică și vibrații | . Technical mechanics and vibrations |
| . Electrotehnică | . Electrotechnics |
| . Ingineria calității | . Quality engineering |
| . Științe fundamentale în inginere civilă | . Fundamental science in civil engineering |

## INFORMATION FOR AUTHORS

- For the works proposed for publication in the Romanian Journal of Civil Engineering, there are no costs for the author to analyze the manuscript and / or publish the article
- The publication of the article is conditional on its analysis in a peer-review process, as mentioned at http://www.rric.ro/etica.php; the author is required to participate in the peer-review process
- The article proposed for publication in the Romanian Journal of Civil Engineering has not been published and can no longer be published in another journal. If portions of content overlap with published content or for publication in another journal, the author must recognize and quote these sources
- Send to publish of an article implies that the study described in the article is original and does not infringe copyright. In the necessary circumstances, the author has to recognize and quote content reproduced from other sources after having previously obtained permission to reproduce the required content from other sources
- If there are more than one author, the content of the article is known and approved by all authors who contributed to writing the article and / or performing the research described in the paper
- All authors of an article should make a significant contribution to its writing
- The proposed article for publication will contain bibliographical references, as well as references to financial support, if any
- In the event of an error being reported in the paper after its publication, the author is required to cooperate with the Editorial Board and the publisher to publish an errata, an addendum, a corrigendum notice, or to withdraw the work if this is considered necessary.

At http://www.rric.ro/template/rric_template.doc there is the template where the proposed article should be sent for publication; the article is sent by email to office@matrixrom.ro or uploaded directly from the journal's website http://www.rric.ro/autori.php.

## INFORMAŢII PENTRU AUTORI

- Pentru lucrările propuse spre publicare în Revista Română de Inginerie Civilă nu există costuri ale autorului pentru analiza manuscrisului şi/sau pentru publicarea articolului
- Publicarea articolului este condiționată de analiza acestuia într-un peer-review proces, așa cum este menționat la http://www.rric.ro/etica.php; autorul este obligat să participe la procesul de peer-review
- Articolul propus pentru publicare în Revista Română de Inginerie Civilă nu a mai fost şi nu mai poate fi publicat într-o altă revistă. Dacă porțiuni de conținut se suprapun cu conținut publicat sau trimis spre publicare la o altă revistă, autorul trebuie să recunoască şi să citeze aceste surse.
- Trimiterea către publicare a unui articol implică faptul că studiul descris în articol este original şi nu încalcă drepturile de autor. În situațiile necesare autorul trebuie să recunoască şi să citeze conținutul reprodus din alte surse, după ce a obținut anterior permisiunea de a reproduce conținutul necesar din alte surse.
- În cazul în care există mai mulți autori, conținutul articolului este cunoscut şi aprobat de toți autorii care au contribuit la scrierea articolului şi/sau la realizarea cercetării descrise în lucrare.
- Toți autorii unui articol trebuie să aibă o contribuție semnificativă la elaborarea acestuia
- Articolul propus pentru publicare va conține referințe bibliografice, precum şi mențiuni referitoare la suportul financiar, dacă este cazul
- În cazul semnalării unor erori în lucrare, după publicarea acesteia, autorul este obligat să coopereze cu Colegiul Editorial şi cu editura pentru a publica o erată, o addendum, o notificare de corrigendum sau pentru a retrage lucrarea, în cazul în care acest lucru este considerat necesar.

La adresa http://www.rric.ro/template/rric_template.doc se gaseste formatul (template) în care trebuie trimis articolul propus pentru publicare; articolul se trimite prin email la adresa office@matrixrom.ro sau se încarcă (upload) direct din website-ul revistei, secțiunea pentru autori http://www.rric.ro/autori.php.